149

External Transmittal Authorized
ORNL
Central Files Number
59-2-65

HIGH FLUX ISOTOPE REACTOR

PRELIMINARY DESIGN STUDY

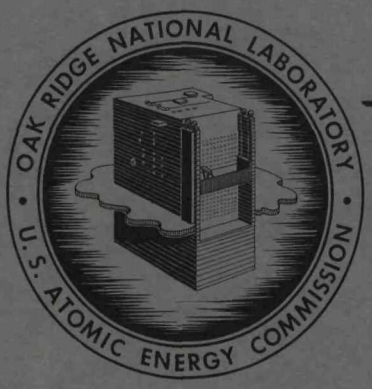

OAK RIDGE NATIONAL LABORATORY
operated by
UNION CARBIDE CORPORATION
for the
U.S. ATOMIC ENERGY COMMISSION

050-001

DISCLAIMER

External Transmittal Authorized
ORNL
Central Files Number
59-2-65

Contract No. W-7405-eng-26

HIGH FLUX ISOTOPE REACTOR

PRELIMINARY DESIGN STUDY

Prepared by

J. A. Lane, Editor
R. D. Cheverton
H. C. Claiborne
T. E. Cole
W. R. Gambill
J. P. Gill
N. Hilvety
J. R. McWherter
D. W. Vroom

DATE ISSUED

OAK RIDGE NATIONAL LABORATORY
Oak Ridge, Tennessee
operated by
UNION CARBIDE CORPORATION
for the
U.S. ATOMIC ENERGY COMMISSION

CONTENTS

HIGH FLUX ISOTOPE REACTOR PRELIMINARY DESIGN STUDY

SUMMARY

A comparison of possible types of research reactors for the production of transplutonium elements and other isotopes indicates that a flux-trap reactor consisting of a beryllium-reflected, light-water-cooled annular fuel region surrounding a light-water island provides the required thermal neutron fluxes at minimum cost. The preliminary design of such a reactor has been carried out on the basis of a parametric study of the effect of dimensions of the island and fuel region, heat removal rates, and fuel loading on the achievable thermal neutron fluxes in the island and reflector. The results indicate that a 12- to 14-cm-dia. island provides the maximum flux for a given power density. This is in good agreement with the USSR critical experiments.

Heat removal calculations indicate that average power densities up to 3.9 Mw/liter are achievable with H_2O-cooled, plate-type fuel elements if the system is pressurized to 650 psi to prevent surface boiling. On this basis, 100 Mw of heat can be removed from a 14-cm-ID × 36-cm-OD × 30.5-cm-long fuel region, resulting in a thermal neutron flux of 3×10^{15} in the island after insertion of 100 g of Cm^{244} or equivalent. The resulting production of Cf^{252} amounts to 65 mg for a $1\frac{1}{2}$-year irradiation. Operation of the reactor at the more conservative level of 67 Mw, providing an irradiation flux of 2×10^{15} in the island, will result in the production of 35 mg of Cf^{252} per 18 months from 100 g of Cm^{244}. A development program is proposed to answer the question of the feasibility of the higher power operation.

In addition to the central irradiation facility for heavy-element production, the HFIR contains ten hydraulic rabbit tubes passing through the beryllium reflector for isotope production and four beam holes for basic research.

Preliminary estimates indicate that the cost of the facility, designed for an operating power level of 100 Mw, will be approximately $12 million.

1. INTRODUCTION

1.1. Historical Background

Review of Requirements. – At a meeting on December 6, 1957, attended by various members of the staff of the Oak Ridge National Laboratory, the possible need for neutron fluxes an order of magnitude higher than presently available, for the production of transplutonium elements and other isotopes, improved research in neutron diffraction, cross section measurements, and solid state physics, was discussed. As a result of this meeting, a series of informal seminars were held to discuss in more detail the need for an ultra high flux research reactor and to review the technical problems associated with the design and construction of such a reactor. Verbatim transcriptions of these seminars have been issued as an ORNL memorandum.[1] The primary conclusion reached in the discussions was that the most pressing need for high thermal neutron fluxes, i.e., $3\text{–}5 \times 10^{15}$ neutrons·cm^{-2}·sec^{-1}, exists in connection with the production of transplutonic elements and other isotopes.

The status of the transplutonic production program received its first serious review at a meeting on January 17, 1958, sponsored by the AEC Division of Research and attended by representatives of the various laboratories interested in the program. At this meeting it was proposed to carry out two different irradiation programs to meet present and anticipated needs for transplutonium isotopes. The

[1] J. A. Lane *et al.*, *Ultra High Flux Research Reactors*, ORNL CF-58-7-117.

first of these involves a sequence of two irradiation, cooling, and processing cycles starting with 10 kg of plutonium in July 1959 which will result in the production of about 1 mg of Cf^{252} by July 1964 and 10 mg of Cf^{252} or less by July 1967. The second program involves the irradiation of 10 g of americium in the MTR to produce 20 μg of Cf^{252} by 1962 and 200 μg by 1964. After a review of these programs by an *ad hoc* committee established to assist the Division of Research with the production and distribution of transplutonium isotopes, the irradiation programs were initiated as proposed.

Although the U.S. transplutonic production program initiated in 1958 seemed to be adequate to meet projected needs, increased interest in the properties of the heavy elements indicated that an even more accelerated production schedule might be advisable. Since any accelerated schedule would require a new isotope production reactor providing thermal neutron fluxes up to 5×10^{15}, a meeting was held in Washington, D.C., on November 24, 1958, to review plans for the construction of such a reactor and other high-flux research reactors. The results of this meeting are summarized in a letter from J. H. Williams to A. M. Weinberg, dated December 12, 1958, a copy of which is included in the Appendix of this report. The unanimous recommendation of those participating in the meeting was that a high flux isotope reactor be designed and constructed at the Oak Ridge National Laboratory with construction to start in fiscal year 1961.

Studies of High Flux Research Reactors. – Numerous studies of high flux research and test reactors have been carried out (see Bibliography) which indicate that an annular fuel region with a central moderating region and a good reflector provides the best geometry for maximizing the thermal flux per unit of power. This is shown in Fig. 1, in which the value of ϕ_{max}/P is plotted against P, where ϕ_{max} is the maximum thermal neutron flux before insertion of an experiment and P is the operating power of the reactor in megawatts. Since the cost of research and test reactors is roughly a function of the power level, internally moderated reactors also provide maximum thermal fluxes for a given cost. This is shown in Fig. 2, which plots the cost and maximum flux in existing and proposed reactors. Figure 2 also shows that the cost of engineering test reactors and their associated facilities is considerably greater than the cost of basic research and isotope reactors with more modest experimental facilities. The characteristics of the reactors shown in Figs. 1 and 2 are summarized in Table 1. It should be pointed out that the maximum thermal neutron fluxes referred to are, in some designs, available over a very limited volume in the reactor.

1.2. The Need for High Thermal Neutron Fluxes

Heavy Element Production. – The production of milligram quantities of americium, curium, berkelium, and californium is important for the development of separations processes for these elements, to study their behavior in existing processes such as Purex, for use as special radiation sources, and to determine their nuclear, chemical, and biological properties. At the thermal neutron fluxes available in existing reactors, however, very long exposure times and large amounts of starting material are required. The irradiation of 10 kg of Pu^{239} at 1.5×10^{14} neutrons·cm^{-2}·sec^{-1} for seven to eight years, for example, results in the production of only 1 mg of Cf^{252}. Fortunately, the production of transplutonic elements in a reactor increases rapidly with increases in neutron flux. This is discussed in the following paragraphs.

The production of transplutonic elements through successive neutron captures in a reactor proceeds according to the following reactions:

$$Pu^{242} + n \longrightarrow Pu^{243} \xrightarrow[5\ hr]{\beta} Am^{243}$$

$$Am^{243} + n \longrightarrow Am^{244} \xrightarrow[26\ min]{\beta} Cm^{244}$$

$$Cm^{244} + 5n \longrightarrow Cm^{249} \xrightarrow[(min)]{\beta} Bk^{249}$$

$$Bk^{249} + n \longrightarrow Bk^{250} \xrightarrow[3\ hr]{\beta} Cf^{250}$$

$$Cf^{250} + 2n \longrightarrow Cf^{252}$$

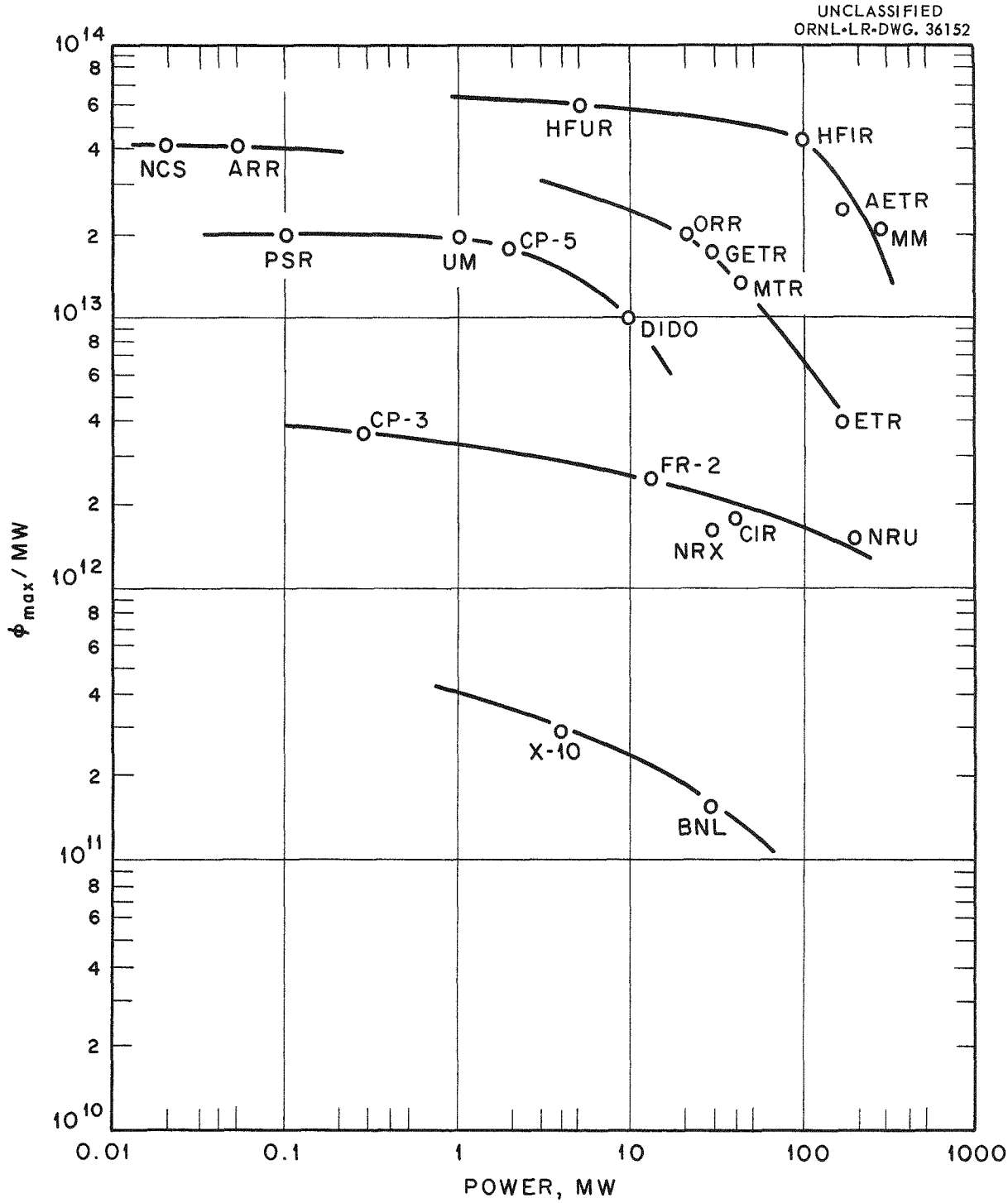

Fig. 1. Maximum Thermal Neutron Flux per Unit Power for Various Reactor Types.

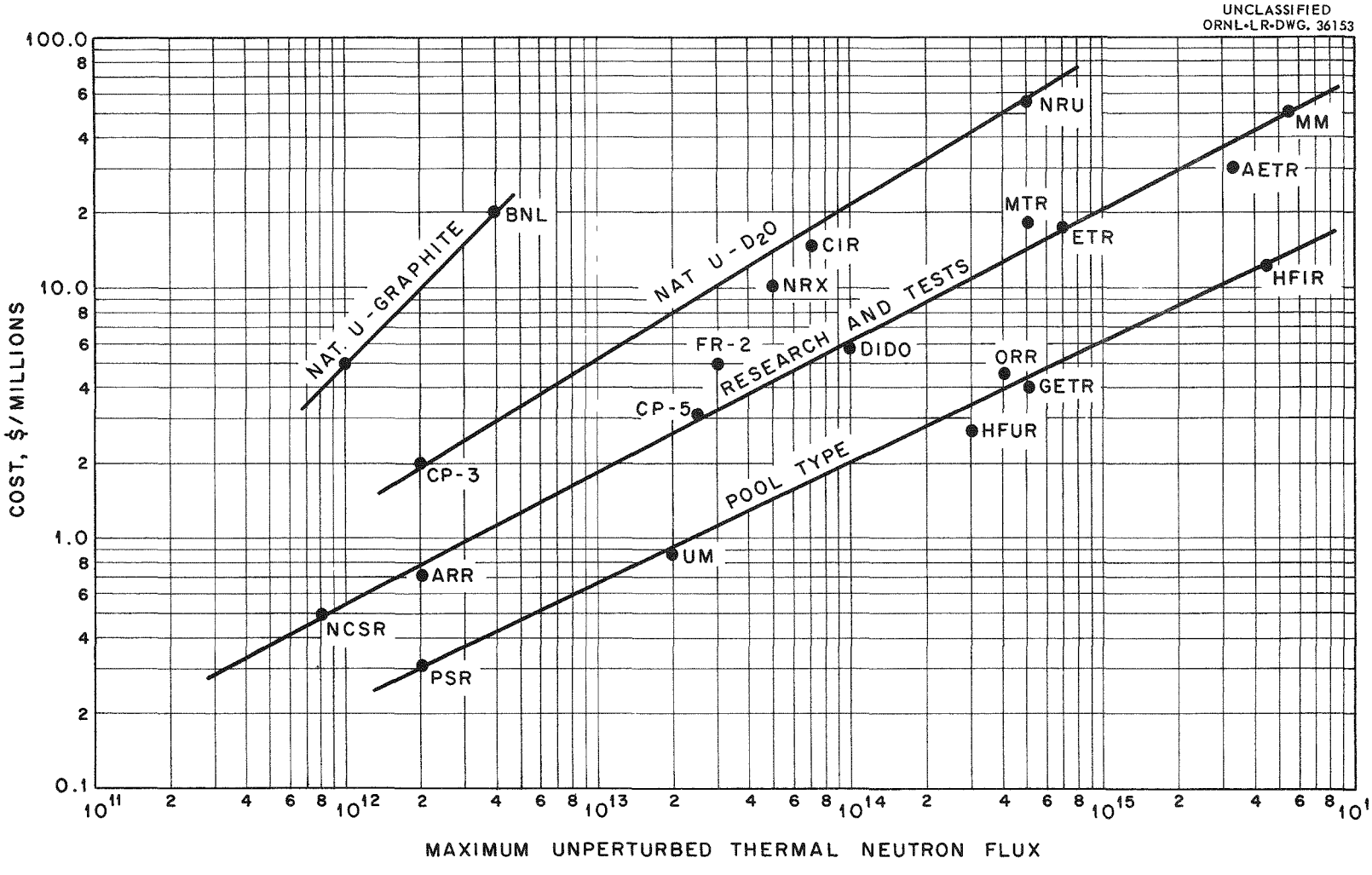

Fig. 2. Cost of Various Reactor Types as a Function of Maximum Thermal Neutron Flux.

Thus, it is seen that ten successive neutron captures are required to produce Cf^{252} from Pu^{242}. Because of this, the *initial* production rate of Cf^{252} from plutonium goes up as the tenth power of the flux. Although this initial rate drops because of burnup of lighter materials and by the approach to equilibrium of some of the high-cross-section intermediates, after a year's irradiation the flux dependence is still somewhere between the second and fourth order.

Similarly, starting with Cm^{244} eight successive captures are required to produce Cf^{252}, also making the production rate extremely flux-dependent. This is shown in Figs. 3 and 4, which give the production of Cf^{252} per gram of Pu^{242} and Cm^{244}, respectively, as a function of time of exposure and thermal neutron flux. It is seen from these figures that a six months' irradiation of 100 g of Pu^{242} at 5×10^{15} flux will produce 10 mg of Cf^{252}, whereas about one year is required to produce the same amount at 3×10^{15} flux. Similarly, 10 mg of Cf^{252} may be produced by irradiating 100 g of Cm^{244} for four months at 5×10^{15} or about six months at 3×10^{15} flux.

Table 1. Characteristics of Existing and Proposed Research Reactors

Reactor	Designation	Power (Mw)	Cost (millions of dollars)	Maximum Unperturbed Thermal Neutron Flux (neutrons·cm^{-2}·sec^{-1})	ϕ_{max}/P
					$\times 10^{13}$
ORNL – graphite	X-10	3.8	5.2	1.1×10^{12}	0.03
Brookhaven – graphite	BNL	28	19.7	4×10^{12}	0.014
Chicago Pile No. 3	CP-3	0.3	2	1×10^{12}	0.67
Karlsruhe Research Reactor	FR-2	12	5.2	3×10^{13}	0.25
Canadian – nat. U–D_2O	NRX	30	10	5×10^{13}	0.17
Canada-India – nat. U–D_2O	CIR	40	15	7×10^{13}	0.18
Canadian – nat. U–D_2O	NRU	200	57	3×10^{14}	0.15
North Carolina State – water boiler	NCS	0.02	0.5	8×10^{11}	4.00
Armour – water boiler	ARR	0.05	0.7	2×10^{12}	4.00
Argonne – heavy water	CP-5	2	3.0	3.5×10^{13}	1.75
Harwell Dido	DIDO	10	5.7	1×10^{14}	1.00
Materials Testing Reactor	MTR	40	18	5×10^{14}	1.25
Engineering Test Reactor	ETR	175	17.2	7×10^{14}	0.40
Advanced Engineering Test Reactor*	AETR	980 (7 cores)	32	3.3×10^{15}	2.40
Mighty Mouse*	MM	250	60	5.5×10^{15}	2.20
Pennsylvania State Reactor	PSR	0.1	0.31	2×10^{12}	2.00
University of Michigan	UM	1	0.85	2×10^{13}	2.00
High Flux University Reactor*	HFUR	5	2.6	3×10^{14}	6.00
Oak Ridge Research Reactor	ORR	20	4.7	4×10^{14}	2.00
General Electric Test Reactor	GETR	30	4	5×10^{14}	1.67
High Flux Isotope Reactor*	HFIR	100	12	4.3×10^{15}	4.30

*Design data only.

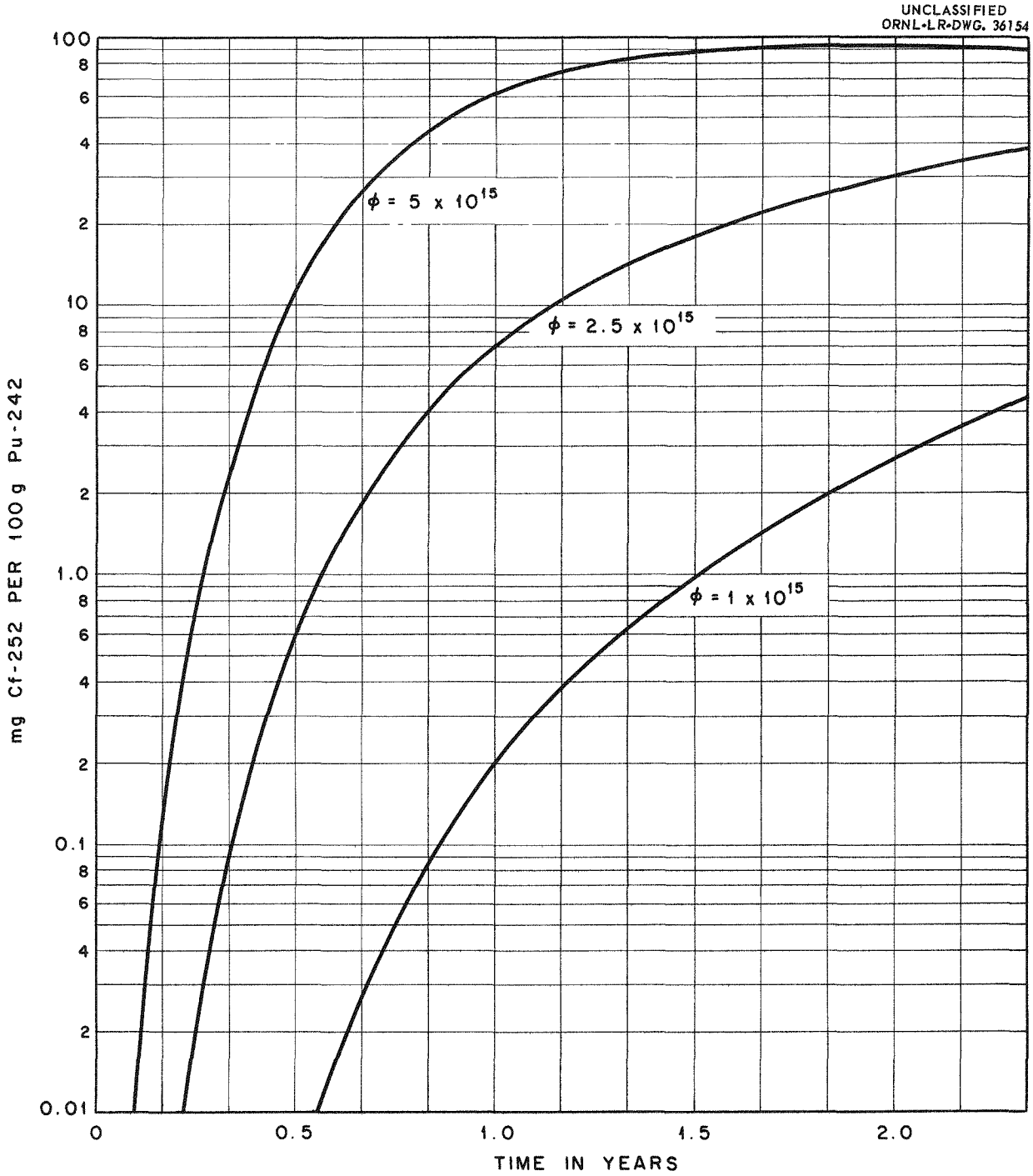

Fig. 3. Production of Cf^{252} from Pu^{242}.

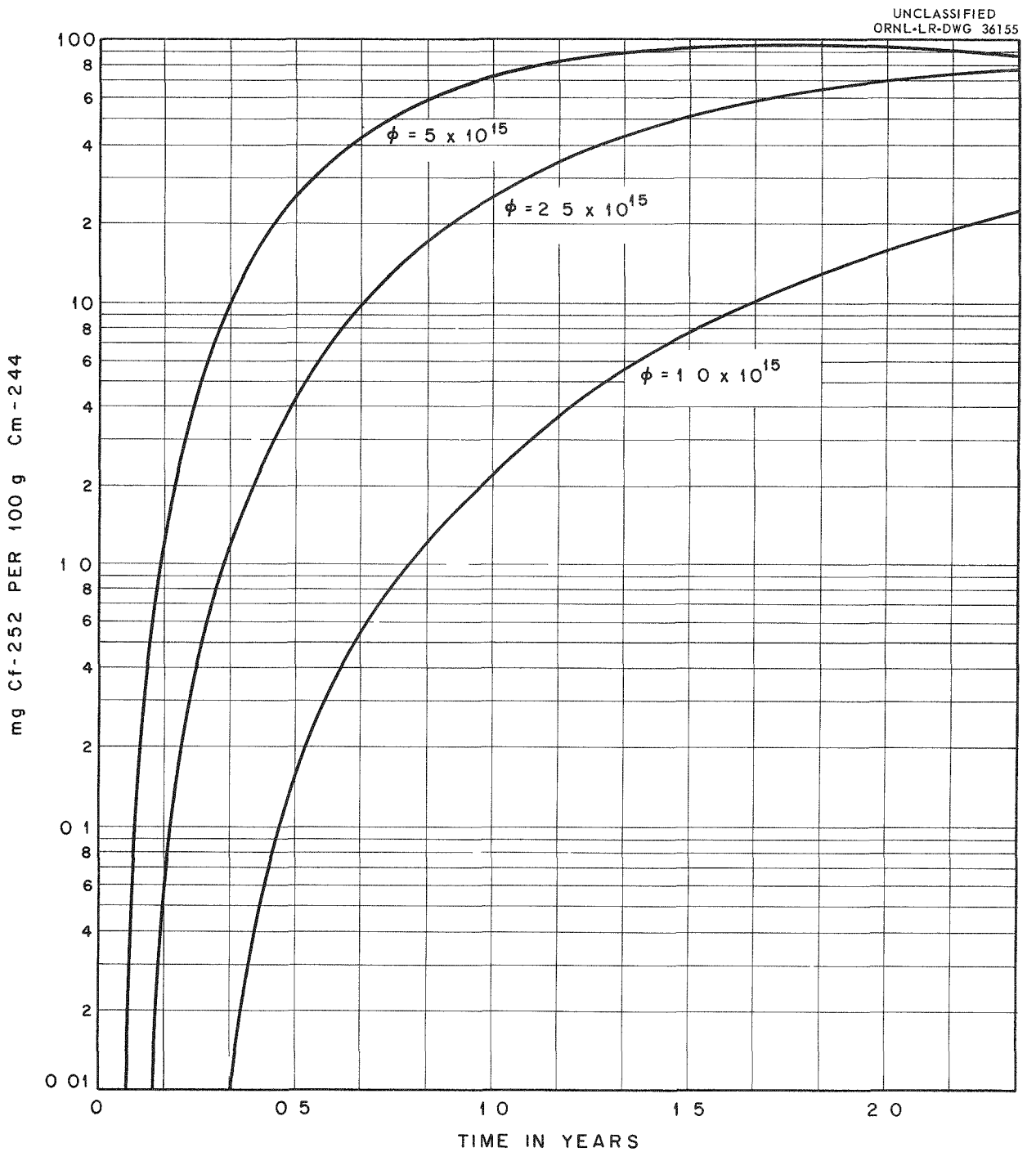

Fig. 4. Production of Cf^{252} from Cm^{244}.

At 1×10^{15} flux, however, a number of years is required to produce this same quantity of Cf^{252}. The incentive for achieving fluxes of 3×10^{15} (after insertion of the material to be irradiated) is very great; however, gains in production time tend to diminish at flux levels higher than this value.

The possibility of increasing the rate of production of Cf^{252} by starting with a larger amount of source material has been examined. Unfortunately, the depression of the thermal flux in the experiment increases with size of sample. Thus there is an optimum sample size to produce the maximum amount of Cf^{252} in a given time. Calculations indicate that 100 g of Cm^{244} will depress the flux about 40%. If it is assumed that the flux depression is proportional to the amount of irradiation material, and that the unperturbed flux in the test hole is 5.0×10^{15}, the optimum quantity of Pu^{242} or Cm^{244} that should be exposed for production of Cf^{252} varies from 75 to 125 g. This is shown in Fig. 5.

In addition to the production of Cf^{252} and other transplutonic elements, the proposed HFIR can be used to produce special isotopes such as Pu^{244}, which can be used to great advantage for certain nuclear research work because of its long alpha half life and zero spin. On account of the short half life of Pu^{243}, only negligible quantities of Pu^{244} can be produced at fluxes below 10^{15} neutrons·cm^{-2}·sec^{-1}, whereas at fluxes of $3–5 \times 10^{15}$ up to 2% of Pu^{242} can be transformed.

The HFIR can also be used to vary the isotopic ratios of certain transuranic elements by burnout of high-cross-section isotopes. Curium, which normally contains up to 95% Cm^{244}, 4% Cm^{246}, and 1% Cm^{245}, is an example of this. By irradiating such a mixture at the available high flux, it is possible to obtain curium which is largely Cm^{248} and which contains little or no Cm^{244}.

The Production of Special Isotopes. – For the production of isotopes of lighter elements, there are a number of reasons why thermal neutron fluxes in the range of 1×10^{15} neutrons·cm^{-2}·sec^{-1} are desirable. These are:

1. the ability to obtain higher specific activities of short-lived isotopes,
2. the speeding-up in the production of long-lived materials,
3. the burning-out of undesired atoms in an isotopic mixture,
4. the conservation of high-cost target materials,
5. the production of carrier-free isotopes, and
6. the reduction in cost of isotopes.

Specific examples of the use of the HFIR for isotopic production are as follows:

1. The production of high-specific-activity short-lived isotopes, such as 12.8-hr Cu^{64}, 14.2-hr Ga^{72}, 12.6-hr I^{130}, 12.5-hr K^{42}, and 15-hr Na^{24}, may be improved by up to a factor of 10 by irradiating the parent atoms at 10^{15} flux instead of 10^{14} flux.

2. The production of long-lived isotopes such as 7.2-year Ba^{133} and 5.3-year Co^{60} may be speeded up by irradiating at higher fluxes. The time to reach the maximum activity of Ba^{133}, for example, is decreased from 19.8 years at 10^{14} flux to 6.6 years at 10^{15} flux. Also, for Co^{60} the time for maximum activity is decreased from 7.8 years to 1.6 years at these two flux levels.

3. The HFIR can also be used to burn out undesired atoms in an isotopic mixture. For example, at 10^{15} flux, 99% of Co^{59} could be burned out of Co^{60} in about five years. Similarly, Eu^{152} and Eu^{154} could be removed from fission product Eu^{155}.

4. Many isotopes are prepared by irradiating isotopically enriched target material, such as Cr^{50} to make Cr^{51}. At 10^{15} fluxes, less target material would be needed; this would reduce the cost of the product.

5. The isotope irradiation facilities in the HFIR can also be used to advantage in producing carrier-free isotopes. For example, Ca^{45}, now made by an n,p reaction with Sc^{45} followed by chemical separation, could be made from Ca^{44} at 10^{15} flux at considerably lower cost.

Neutron Beam Research. – Although the HFIR is intended primarily for isotope production, the design will incorporate four 4-in.-dia horizontal beam holes for neutron diffraction experiments and cross-section measurements. Estimated thermal fluxes at the face of these beam holes are $3–5 \times 10^{14}$ with the control rods in and $6–9 \times 10^{14}$ with the control rods out.

Solid State Physics. – The fast flux in the fuel region of the HFIR will be about 4.7×10^{15} at full-power operation. Materials can be irradiated in this region to carry out accelerated radiation damage studies. The available flux will be of

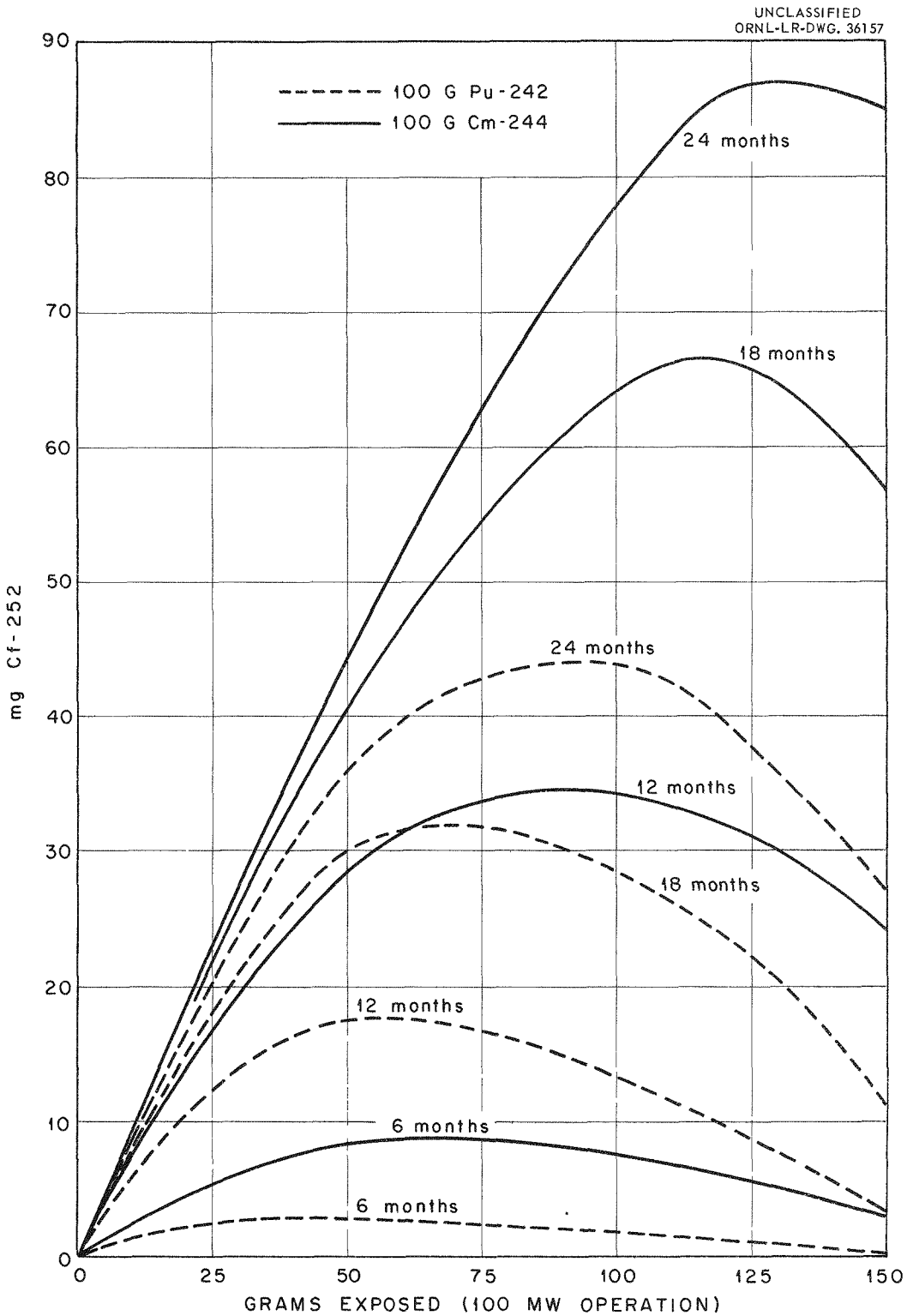

Fig. 5. Production of Cf^{252} as a Function of Weight of Starting Material.

particular interest in determining the effect of radiation on the mechanical properties of metals and ceramics used in power reactors. Studies of solid state reactions and neutron diffraction experiments with metals can also be done expeditiously in the facilities and fluxes available in the HFIR.

Achievable Thermal Neutron Fluxes. – It is seen from the foregoing that thermal neutron fluxes in the range of $2–3 \times 10^{15}$ are desired for the production of heavy elements and 1×10^{15} for the production of other isotopes. In regard to the former, operating power levels of 100 Mw and maximum power densities up to 7200 kw/liter must be achieved to obtain an effective thermal neutron flux of 3×10^{15} in a 100-g sample of Cm^{244}. It is believed that while such conditions may push the technology of water-cooled reactors to their practical limit, operation of the reactor at two-thirds of its design power results in quite conservative conditions. A comparison of the production of Cf^{252} from Cm^{244} at these two levels is shown in Fig. 6.

1.3. Physics of Flux-Trap Reactors

Critical Experiments. – Critical experiments on flux-trap configurations have been made at ORNL and in the USSR. Although the configurations tested were not identical with the proposed design, they do indicate the feasibility of obtaining very high thermal neutron fluxes in flux-trap reactors. With no regard to power density limitations, the ORNL results extrapolate to an unperturbed thermal neutron flux of 3.8×10^{15} at 100 Mw and the Russian results to 4.4×10^{15}.

Some preliminary critical experiments were made in the ORR with flux-trap configurations. Initial results[2] show that a flux peaking (ratio of maximum flux in trap to average flux in fuel) of 4 resulted from loading fuel in the form of a hollow square, five elements on a side, enclosing a square array of nine beryllium pieces. Flux measurements indicate that the maximum unperturbed thermal flux in the beryllium island would be 3.8×10^{15} when extrapolated to 100-Mw operation. Subsequent calculations and Russian experiments show that the tested configuration was not optimum.

A paper on a high flux research reactor utilizing the flux-trap principle was presented at Geneva by Feinberg *et al.*[3] The paper was primarily devoted to a description and results of critical experiments that were required to determine the nuclear characteristics of the engineering design. Based on the critical experiments, a maximum unperturbed flux of 2.2×10^{15} at 50 Mw is claimed for the Russian design.

The Russian experiments were quite extensive and included a study of the effect of moderator-to-uranium ratio, geometry (including water island), structural material, and reflector materials on critical mass, critical volume, and flux distribution. Efficiencies of fuel blocks and control rod worth at design positions were also determined. A notable omission in the paper is the determination of the temperature coefficient of reactivity.

Over a wide range of variables, it was found that an H/U^{235} ratio between 30 and 40 gave a minimum critical volume. Structural materials tested included aluminum, stainless steel, nickel, and copper. Each atom of parasitic material per atom of U^{235} resulted in about a 7.5% increase in critical volume. Geometry effects studied included approximately circular and cruciform fuel arrangement, flux-trap dimension, and fuel plate spacing. Reflector materials investigated were beryllium oxide, water, graphite, cast iron, steel, natural-uranium–water mixtures, and thorium-water mixtures. A beryllium oxide reflector was found to reduce the critical volume and mass by more than 50% as compared with a pure water reflector.

Neutron flux distributions were determined throughout the various configurations by copper activation, indium activation, and cadmium ratio measurements. For the systems approximating the final design, trans-cadmium fissions were approximately 50%, which demonstrates that efficient flux-trap reactors are essentially epithermal.

Some comparisons are made with calculations and experimental results for configurations containing no flux trap. It is claimed that the calculated flux distributions are satisfactory, although the calculated critical masses are low by 1 to 33% depending on the particular conditions. The calculational method used was the P_1 approximation with 19 energy groups.

The extensive experimental studies by the Russians should be very helpful in planning and reducing the number of required critical experiments for the ORNL design.

[2] F. T. Binford, "Flux Trap Tests," *Operations Division Quarterly Report, July–September, 1958*, ORNL CF-58-9-88.

[3] S. M. Feinberg *et al.*, *An Intermediate Reactor for Obtaining High Intensity Neutron Fluxes*, Geneva Conference Paper 2142, August 12, 1958.

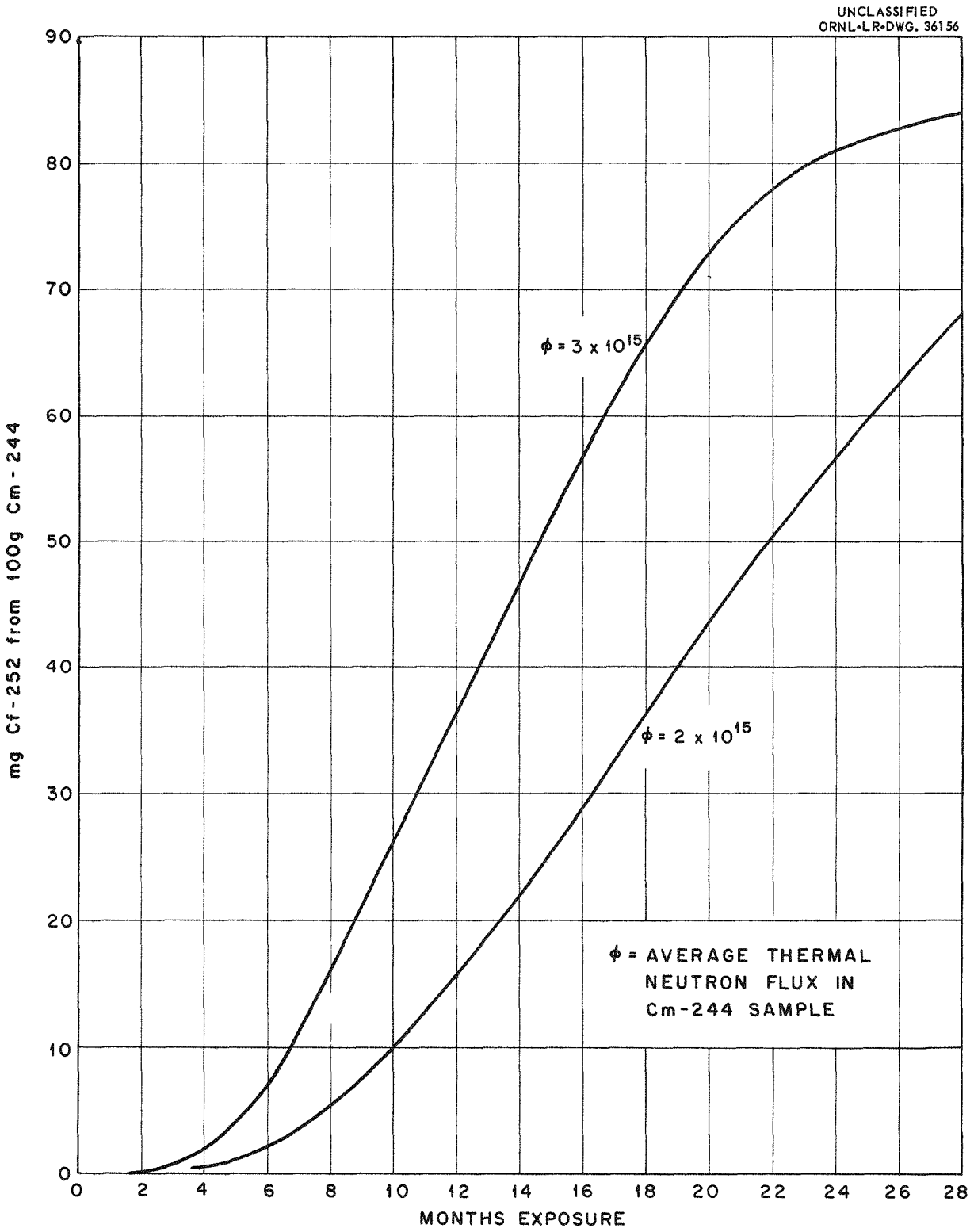

Fig. 6. Production of Cf^{252} at Various Fluxes.

2. DESCRIPTION OF FACILITY

2.1. General Characteristics

The HFIR characteristics given in Tables 2 and 3 are based upon the nuclear and heat transfer parameter studies. The goal of these studies, discussed in Sec 1.2, was to obtain a reasonably optimum reactor design capable of producing an average perturbed flux of 3×10^{15} thermal neutrons·cm^{-2}·sec^{-1} in a 100-g Cm^{244} sample at a power level of 100 Mw. Since the initial operation of the reactor may be at less than design conditions, two sets of characteristics are listed in Table 2: a set of design values, and a second set of possible initial operating values.

2.2. Optimization Studies

Nuclear Calculations. – The principle of the flux trap has been used for this design study so that the high thermal flux will be obtained in a region other than the fuel region. The peaking of the thermal flux in the central moderator region or trap and also in the reflector surrounding the fuel annulus results from moderation of the fast leakage from the fuel region. Therefore, in order to increase the thermal peaking, the fast leakage from the fuel annulus should be increased and optimum moderation in the trap and reflector provided. Thus, the primary purpose of the nuclear calculations was to determine the optimum size and composition of a reactor core cooled by light water and moderated and reflected by light water and beryllium.

For purposes of investigating the effects of various reactor parameters on the peaking of the thermal flux, two-group and thirty-three-group multiregion diffusion theories were used. Since the optimum core size is small, requiring a high fuel concentration, an appreciable number of fissions occurs with nonthermal neutrons. Therefore, for the two-group model an averaged fast-group fission cross section, based on the U^{235} resonance integral, was included. All the fast constants for the two-group calculations were averaged, assuming a $1/E$ neutron flux energy distribution. The value of the age used in calculating the fast removal cross section in the fuel region was obtained from empirical relations based on experimental age measurements in water-aluminum mixtures. The age for water at 80°C was considered to be 33 cm^2.

The two-group calculations were performed on an IBM-704 computer, using WANDA, a one-dimensional, multigroup-multiregion diffusion theory code. The thirty-three-group calculations were performed on the same computer, using GNU-II, a similar code that includes the Selengut-Goertzel term for neutron slowing-down in hydrogen. Fast constants for GNU-II were averaged, assuming a $1/E$ neutron energy distribution in each group. As yet, only one GNU-II case has been run. It indicates a 10% higher thermal neutron flux in the experiment per unit reactor power than obtained with WANDA calculations.

The basic core geometry investigated was a right cylinder made up of several concentric annular regions comprising the flux trap, fuel region, and beryllium reflector, respectively. The flux trap was assumed to contain the material to be irradiated plus a sufficient amount of aluminum carrier to provide the necessary heat transfer surface area, an area adjacent to the central experiment containing varying amounts of beryllium and water, and a region of light water located between this area and the fuel annulus. A beryllium reflector surrounding the fuel annulus contained 5% by volume of cooling water and enough poison to represent experiments in the reflector. The fuel annulus consisted of fully enriched uranium-aluminum fuel plates and enough light water coolant-moderator to provide a metal-to-water ratio of 1.

At each end of the cylindrical core 8 cm of reflector savings were added, as compared with 9 cm measured in the MTR.[4]

A schematic representation of the general reactor core and the neutron flux spatial distributions therein are shown in Fig. 7.

Core Physics. – *Limitations on Maximum Thermal Neutron Flux.* – Once a reactor core design has been selected, the maximum attainable thermal neutron flux is limited by the desired power level, the maximum permissible power density, and an adequate minimum fuel cycle time, the latter value being essentially a direct function of the power density. For this particular reactor the upper limit on power was fixed primarily on the basis of capital costs. The maximum permissible power density, which ultimately is limited by burnout

[4] M. L. Batt *et al.*, *Reflector Savings Due to the MTR Water Blanket*, IDO-16075 (1953).

considerations, was also limited by the fuel plate surface temperature and therefore the desirable system pressure. Thus, particularly for cores employing subcooled heat transfer, the core design must be carefully optimized from a nuclear standpoint.

Regardless of the set upper limit on reactor power level, economy in capital and operating costs requires that for a given average neutron flux in the experiment the core power should be as low as possible. Therefore the quantity ϕ/P, defined as the volume-averaged thermal flux in the central experiment per unit of reactor power, is of significance and should be maximized by the proper choice of region diameters, core length, fuel concentration, moderator composition, etc.

Table 2. Nuclear and Heat Transfer Characteristics

Characteristics	Design	Initial Operation
Nuclear		
Reactor power, Mw	100	67
Average thermal flux in sample (100 g Cm^{244}), neutrons·cm^{-2}·sec^{-1}	3.0×10^{15}	2.0×10^{15}
Average thermal flux in sample per unit of power, neutrons·cm^{-2}·sec^{-1}·Mw^{-1}	3.0×10^{13}	3.0×10^{13}
Maximum unperturbed thermal flux in island	5.1×10^{15}	3.4×10^{15}
Maximum fast flux in fuel region	4.7×10^{15}	3.1×10^{15}
Maximum thermal flux at beam holes in outer reflector with control rods in	5.0×10^{14}	3.3×10^{14}
Maximum unperturbed thermal flux in outer reflector	9.5×10^{14}	6.3×10^{14}
Fuel cycle time for $k_{eff} = 1.183$, days	10	15
Heat removal		
Specific power, Mw per kg of U^{235}	28.6	19.2
Maximum power density, Mw/liter	7.2	4.8
Average power density, Mw/liter	3.9	2.6
Maximum heat flux, Btu·hr^{-1}·ft^{-2}	2.3×10^{6}	1.55×10^{6}
Average heat flux, Btu·hr^{-1}·ft^{-2}	1.26×10^{6}	0.84×10^{6}
Burnout heat flux, Btu·hr^{-1}·ft^{-2}	5.3×10^{6}	5.5×10^{6}
Heat transfer surface area, ft^2	270	270
Ratio of maximum to average power density (total)	1.84	1.84
Ratio of maximum to average power density (radial)	1.2	1.2
Ratio of maximum to average power density (axial)	1.2	1.2
Ratio of maximum to average power density (uncertainty)	1.28	1.28
Engineering hot spot and hot channel factors	1.33	1.33
Maximum surface temperature, °F	450	352
Coolant inlet temperature, °F	120	120
Coolant outlet temperature, °F	195	170
Coolant velocity, fps	45	45
Coolant circulation rate (fuel region), gpm	9400	9400
Pressure drop across core, psi	84	84
System pressure at pump discharge, psi	650	650

The maximum ϕ/P obtained in the above manner may not, however, be compatible with heat removal requirements in the fuel annulus. As the various reactor parameters are varied, the ratio of maximum to average power density or surface heat flux in the fuel region varies, as well as the volume of the fuel region. On the other hand, once the fuel plate thickness, coolant channel thickness, maximum surface temperature, coolant velocity, etc., are fixed, the allowable maximum power density is established, independently of the nuclear reactor parameters. Therefore, a maximum ϕ/P is not sufficient to guarantee a desired neutron flux, since the resultant necessary power density may very well exceed the allowable.

To alleviate the above condition another ratio, $\phi/(P/V)_{m'}$ has been defined as the volume-averaged flux in the central experiment per unit of maximum power density. This quantity contains the radial and axial maximum to average power densities and an engineering factor to account for variations in heat transfer parameters from the nominal values. Thus, once the allowable maximum power density has been established, the nuclear parameters must be adjusted to obtain a $\phi/(P/V)_m$ that will produce the desired thermal flux in the experiment.

Variation of $\bar{\phi}_{21}/(P/V)_m$ with Reactor Parameters. – The values of $\bar{\phi}_{21}/(P/V)_m$ were obtained

Table 3. General Characteristics

Core design and size	
Type of core	Cylindrical annulus, flux trap
Type of fuel elements	Aluminum plates or tubes
Fuel plate thickness, in.	0.040
Coolant channel thickness, in.	0.040
Metal-to-water ratio in fuel annulus	1
Length of active core, cm	30.5
Inside diameter of fuel annulus, cm	14
Outside diameter of fuel annulus, cm	36
Volume in fuel annulus, liters	26.3
Diameter of central experiment, cm	4
Outside diameter of outer reflector, cm	96
Core materials	
Fuel	Enriched uranium (~90%)
Fuel loading (for aluminum fuel elements), kg of U^{235}	3.5*
Fuel loading (for stainless-steel-clad elements), kg of U^{235}	12.2
U^{235} concentration in fuel annulus (5 adjacent regions across width of plate), atoms/cm^3	
Region 1	20.00×10^{19}
Region 2	33.90×10^{19}
Region 3	39.44×10^{19}
Region 4	39.80×10^{19}
Region 5	31.26×10^{19}
Outer reflector material	Beryllium + 5% H_2O
Island moderator-reflector material	Light water
Coolant	Light water

*May be 30% low based on USSR data.

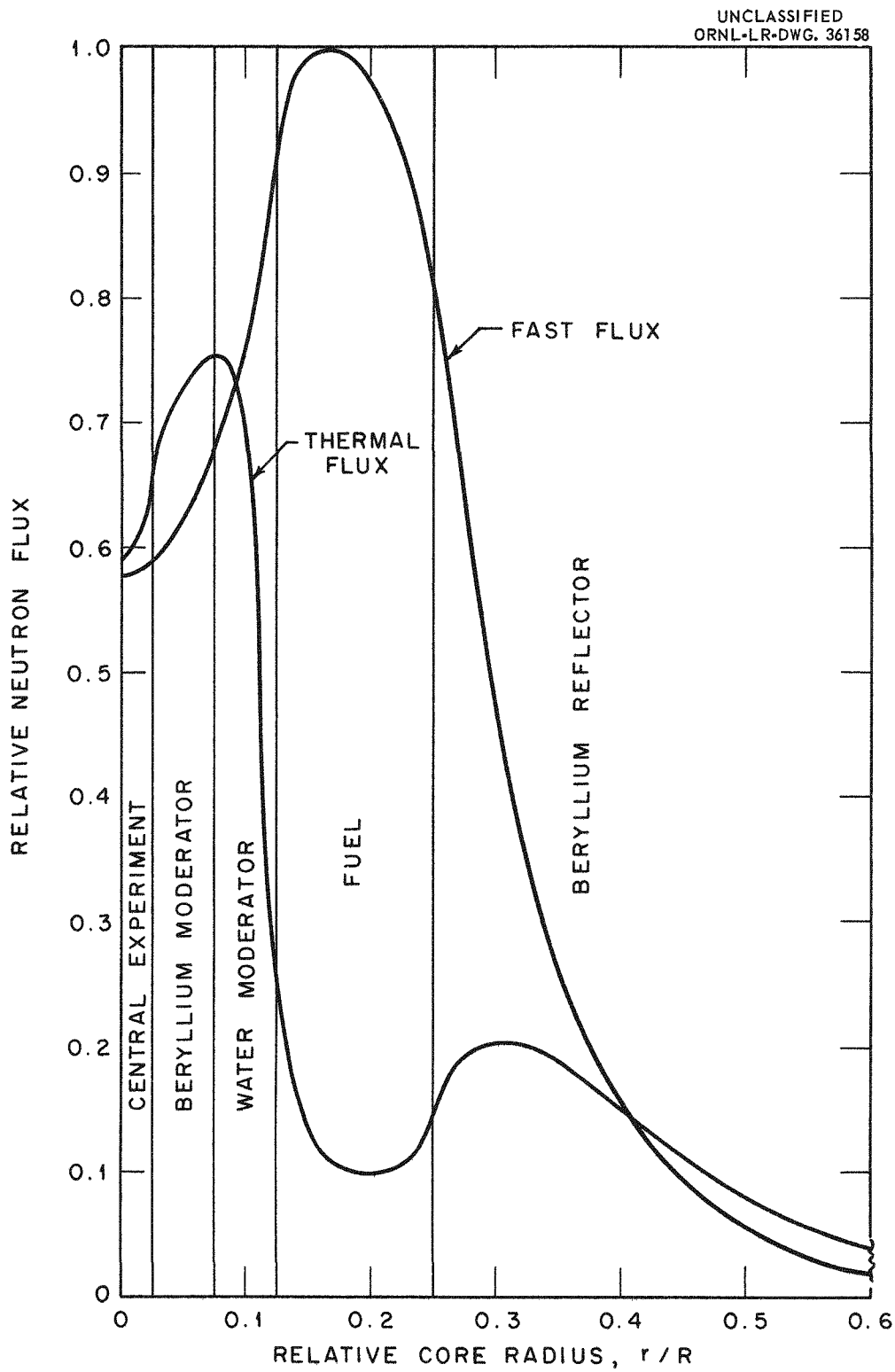

Fig. 7. Schematic Representation of HFIR Core and Typical Spatial Neutron Flux Distribution.

from

$$\frac{\bar{\phi}_{21}}{(P/V)_m} = \frac{w}{\frac{q_{max}}{q_{av}}\left(\Sigma_{f2}\frac{\bar{\phi}_{2F}}{\bar{\phi}_{21}} + \Sigma_{f1}\frac{\bar{\phi}_{1F}}{\bar{\phi}_{21}}\right)},$$

where

$$\frac{q_{max}}{q_{av}} = \frac{\phi_{2F}}{\bar{\phi}_{2F}}\,\frac{\sigma_{f2} + (\phi_{1F}/\phi_{2F})\,\sigma_{f1}}{\sigma_{f2} + (\bar{\phi}_{1F}/\bar{\phi}_{2F})\,\sigma_{f1}} \times \left(\frac{q_{max}}{q_{av}}\right)_{axial} \times \left(\frac{q_{max}}{q_{av}}\right)_{uncertainty},$$

$\bar{\phi}_{21}$ = volume-averaged thermal flux in region 1 (experiment),

$(P/V)_m$ = maximum power density, obtained by multiplying the average power density by the radial, axial, and "uncertainty" ratios of maximum to average power densities,

q_{max}/q_{av} = ratio of maximum to average power density or heat flux,

$\bar{\phi}_{2F}$ = average thermal flux in fuel,

$\bar{\phi}_{1F}$ = average fast flux in fuel,

ϕ_{2F}, ϕ_{1F} = corresponding (same radial position) values of thermal and fast fluxes, respectively, in the fuel which result in the largest value of q_{max}/q_{av} (they are usually at one of the two boundaries),

Σ_{f2}, Σ_{f1} = macroscopic thermal and fast fission cross sections in fuel, respectively,

σ_{f2}, σ_{f1} = microscopic thermal and fast fission cross sections in fuel, respectively,

N^{25} = U^{235} atom concentration in the fuel annulus (assumed homogenized),

w = energy per fission, wsec.

Since the thermal terms in the above expressions predominate, the value of $(1/N^{25})(\bar{\phi}_{21}/\bar{\phi}_{2F})$ should be made as large as possible, and $\phi_{2F}/\bar{\phi}_{2F}$ should be reduced as close to unity as possible. For given values of N^{25} and fuel annulus thickness, $\bar{\phi}_{21}/\bar{\phi}_{2F}$ has a maximum value for an optimum value of central reflector-moderator island radius. Too large an island provides excessive neutron absorption, while too small an island does not provide adequate moderation. Increasing the fuel concentration increases $\bar{\phi}_{21}/\bar{\phi}_{2F}$, since the fast neutron leakage from the fuel region increases. However, for a given fuel annulus thickness there is an optimum island radius that results in a minimum fuel concentration for a given value of k_{eff}. The conflicting trends suggested that a maximum value of $\bar{\phi}_{21}/(P/V)_m$ might occur for an optimum island radius and fixed values of fuel annulus thickness and k_{eff}. Figure 8 shows this to be the case, the optimum island radius being about 7 cm and essentially independent of the fuel annulus thickness for the cases indicated. The curves also indicate that increasing the fuel annulus thickness increases $\bar{\phi}_{21}/(P/V)_m$.

Figure 9 shows that q_{max}/q_{av} also has a maximum value for an island radius of about 7 cm. The large value of q_{max}/q_{av}, calculated for uniform fuel distribution in the fuel annulus, indicated some advantage could be gained by reducing the value to nearly 1. Since one conception of the fuel annulus design included essentially radial fuel plates, it was postulated that radial variations in fuel concentrations be made so as to flatten the radial power density distribution. The lower curve in Fig. 9 indicates that q_{max}/q_{av} can be reduced significantly by using five distinct fuel regions in the fuel annulus.

To cope with the problem of excessive absorption in a large H_2O island, investigations were made replacing a central portion of the H_2O island with beryllium. Typical results are shown in Fig. 10, indicating that over a certain range of island radii there is an optimum combination of beryllium and water that will produce a maximum value of $\bar{\phi}_{21}/(P/V)_m$ for a given fuel annulus thickness. For small island radii no beryllium is required, and for large islands all beryllium is required. [The cores used in Figs. 8, 9, 11, and 12 include no beryllium in the island. Optimum beryllium-water islands would make the right-hand portion of the curves in Figs. 8 and 12 considerably flatter, but for an island radius of 7 cm there would be essentially no change in $\bar{\phi}_{21}/(P/V)_m$.]

Another possible method of increasing the average thermal flux per unit of power in the central experiment is illustrated in Fig. 11. The curves indicate that for a given core size and weight of material to be irradiated, there is an optimum

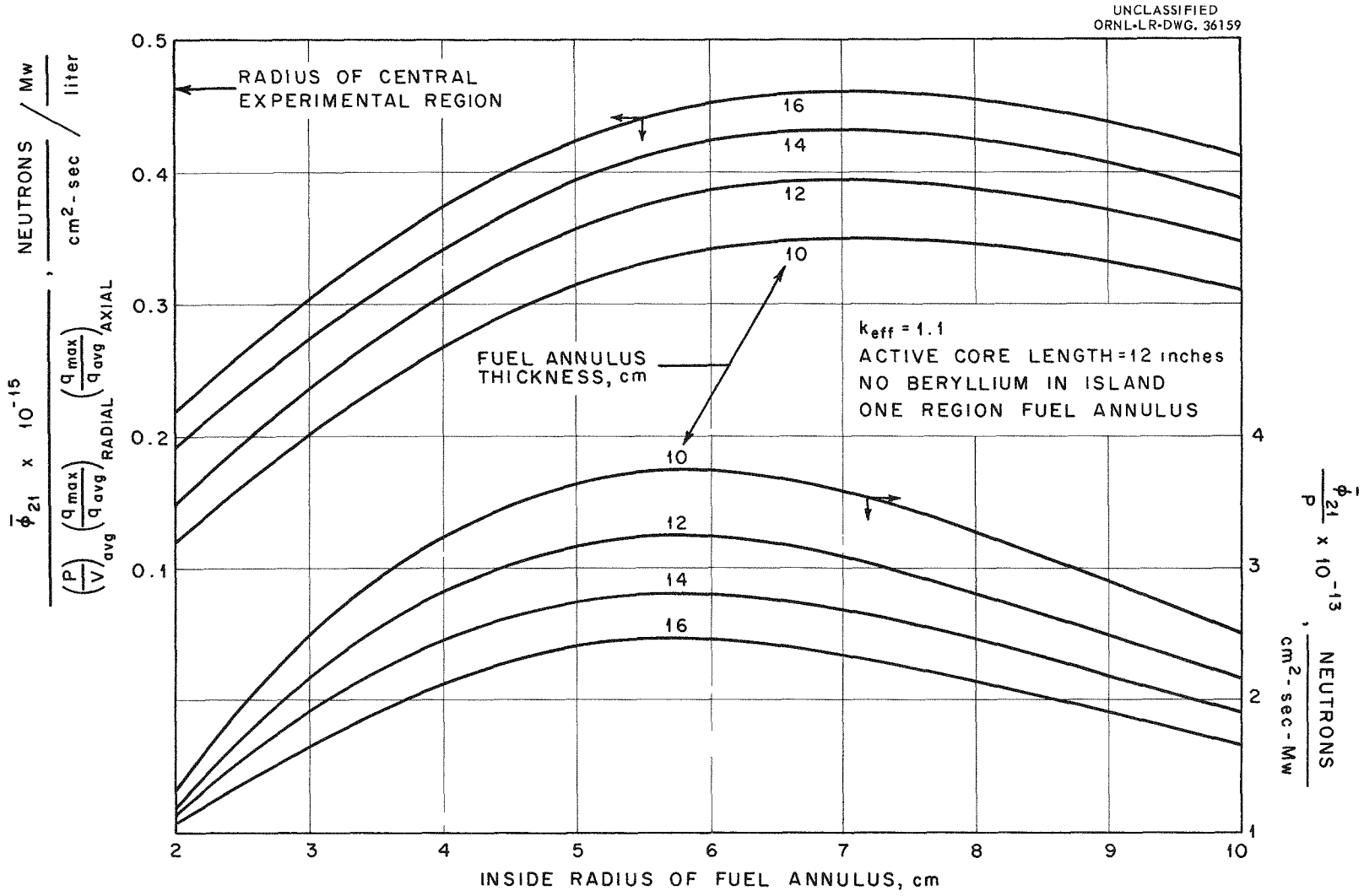

Fig. 8. Average Thermal Flux in Experiment per Unit Power Density and per Unit Power as a Function of the Inside Radius and the Thickness of the Fuel Annulus.

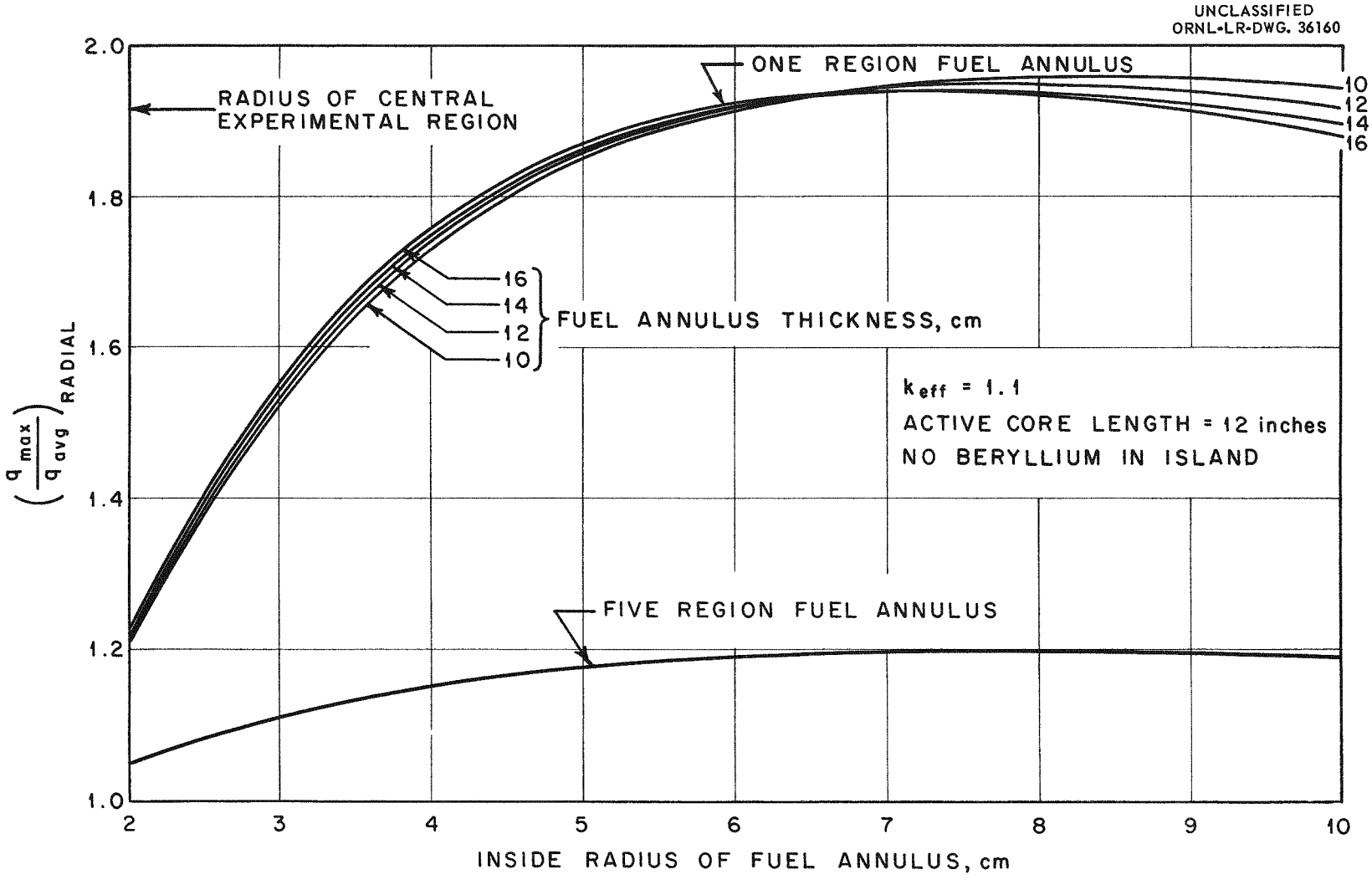

Fig. 9. Radial Maximum to Average Power Density as a Function of the Inside Radius of the Fuel Annulus for One- and Five-Region Annuli.

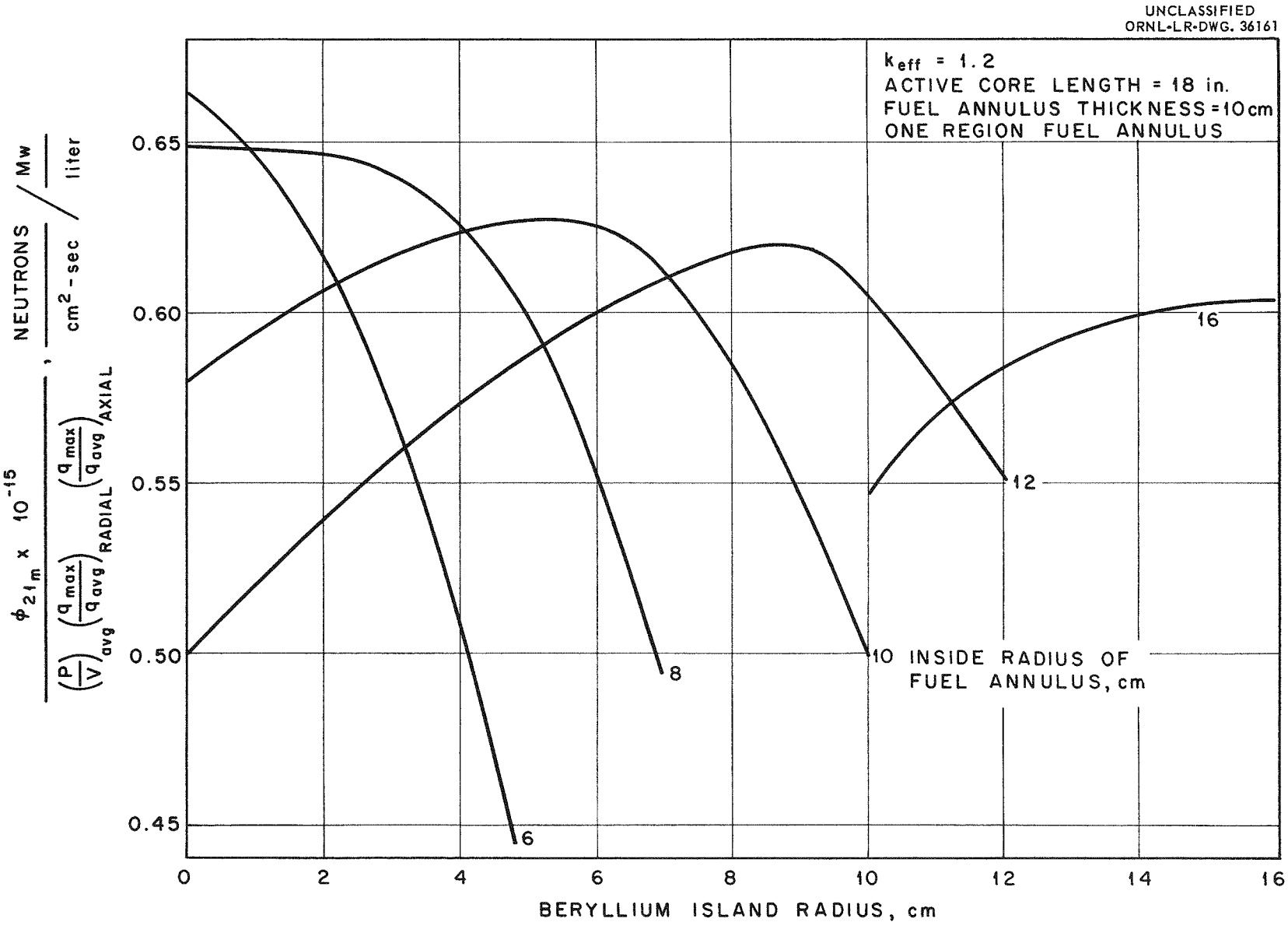

Fig. 10. Maximum Unperturbed Thermal Flux per Unit Power Density in Experimental Facility as a Function of the Beryllium Island Radius and the Fuel Annulus Inside Radius.

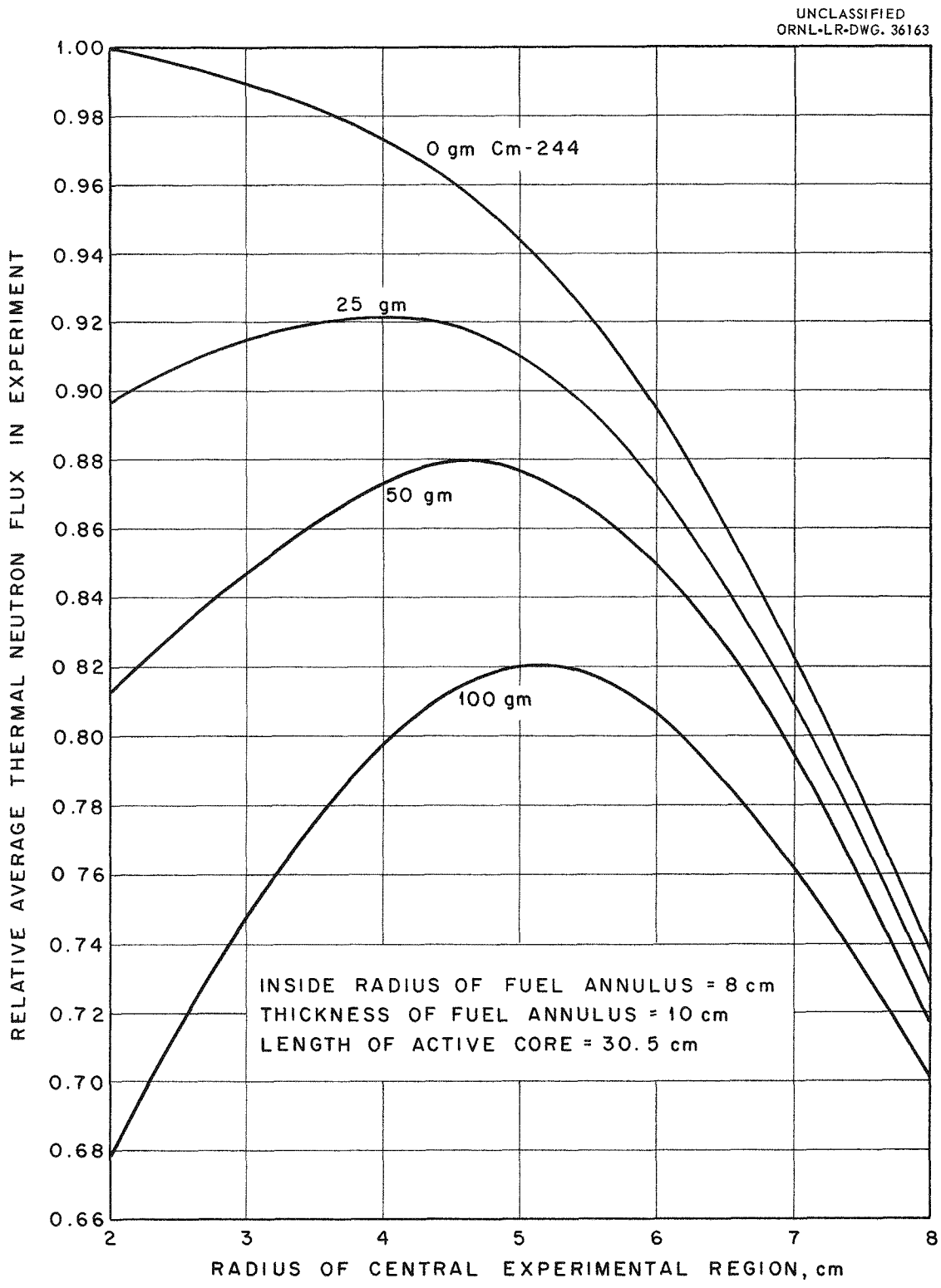

Fig. 11. Average Thermal Neutron Flux in the Experiment as a Function of the Experimental Region Radius and the Weight of Cm^{244} Dispersed in the Experimental Region.

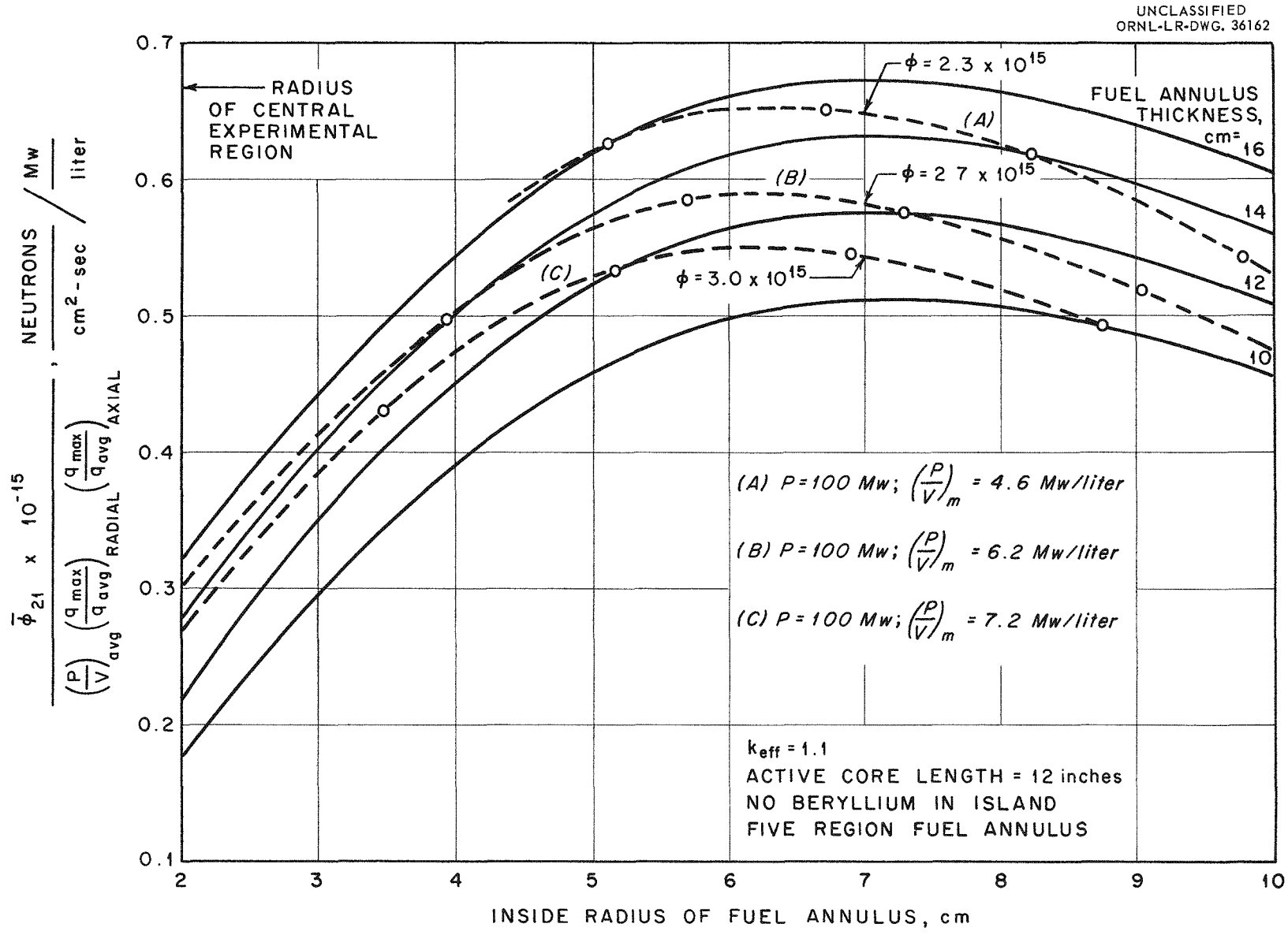

Fig. 12. Average Thermal Flux in Experiment per Unit Power Density as a Function of the Inside Radius and the Thickness of the Fuel Annulus.

radius of the experimental region which will produce a maximum average flux. For an experiment containing 100 g of Cm^{244}, about 20% increase in flux can be achieved by increasing the radius of the experimental region from 2 to 6 cm.

The maximum values of $\bar{\phi}_{21}/P$ and $\bar{\phi}_{21}/(P/V)_m$ do not necessarily occur with cores having the same island radius, as shown in Fig. 8. However, if constant power curves are superimposed on the $\bar{\phi}_{21}/(P/V)_m$ curves, as shown in Fig. 12, the optimum radii for maximum $\bar{\phi}_{21}/(P/V)_m$ and $\bar{\phi}_{21}/P$ and minimum fuel concentration are very nearly the same, being about 6 cm.

For the "optimum" HFIR design included in this report, an inside radius of 7 cm was tentatively selected for the fuel annulus because it provided more experimental space in the island and allowed a thinner fuel annulus for the same fuel volume. As seen in Fig. 12 there is little difference in flux for the 6- and 7-cm islands.

Heat Transfer in Core. – From the standpoint of heat transfer the maximum attainable thermal flux is limited by the permissible maximum power density or, more specifically, the heat flux in the fuel annulus. Before actual burnout tests are conducted on HFIR-type fuel plate assemblies, the ratio between burnout heat flux and maximum design heat flux (as defined in this report) is fixed on the basis of the accuracy with which the burnout heat flux can be calculated. However, the ratio of design thermal neutron flux to burnout thermal neutron flux can be increased as the uncertainty factor in the calculation of the heat transfer coefficient for subcooled forced convection is decreased.

The correlation of heat transfer coefficient selected for the fuel plates was that recently proposed by Levy *et al.*,[5] which is based on data for water flowing vertically in thin rectangular channels (100-mil gap) at high velocity (up to 50 ft/sec) and nonboiling heat fluxes up to 1×10^6 $Btu \cdot hr^{-1} \cdot ft^{-2}$. The heat transfer coefficients obtained were considerably smaller than those predicted by the standard Sieder-Tate, Dittus-Boelter, or Colburn equations; they may be represented for the present region of interest (and approximately for $15{,}000 < N_{Re} < 200{,}000$) by

$$(N_{Nu})_b = 0.09\,(N_{Re})_b^{0.654}\,(N_{Pr})_b^{1/3}\,(\mu_b/\mu_s)^{0.14},$$

where

$$N_{Nu} = hd/k,$$
$$N_{Re} = d\rho v/\mu,$$
$$N_{Pr} = c_p\mu/k,$$

subscript b denotes evaluation at bulk water temperature, and subscript s denotes evaluation at surface temperature.

As compared with the test sections used by Levy, the coolant gap of the present design is only 0.4 as large, and the channel aspect ratio is eightfold larger. Nevertheless, the above equation represents the best approximation available for the presently contemplated HFIR design conditions.

At a Reynolds number of about 70,000 the Levy equation yields a film coefficient about 25% less than the Sieder-Tate equation and an even greater percentage less than the Colburn and modified Colburn equations.

For a given heat flux the power density is increased by decreasing the thickness of the fuel plate and coolant channel. Also, h is increased by decreasing the coolant channel thickness. Therefore the two dimensions were made as small as was considered practical from the standpoint of fabrication, strength, and dimensional stability. The coolant velocity between the plates was then made as high as appeared reasonable.

Using fuel plates and coolant channels as thin as those considered for this reactor, one must be very cautious in selecting appropriate values for hot spot and hot channel factors. For the calculations presented in this report it was assumed that the hot channel and hot spot factors were equal. The value used was estimated by modifying hot spot and hot channel factors obtained for the ETR.[6] The fraction of the conventional hot spot and hot channel factors that reflects the uncertainty associated with the determination of the over-all maximum to average power density was factored out so that

$$\left(\frac{P}{V}\right)_m = \left(\frac{P}{V}\right)_{av} \times \left(\frac{q_{max}}{q_{av}}\right)_{radial} \times \left(\frac{q_{max}}{q_{av}}\right)_{axial} \times \left(\frac{q_{max}}{q_{av}}\right)_{uncertainty},$$

[5] S. Levy, R. A. Fuller, and R. O. Niemi, *Heat Transfer to Water in Thin Rectangular Channels*, Am. Soc. Mech. Engrs., Paper No. 58-A-127 (1958).

[6] V. A. Walker, IDO-16461.

where the radial and axial terms were determined from the calculated spatial fission distribution in the fuel region. The remaining fraction of the conventional hot spot and hot channel factors was considered to be the ratio of maximum to nominal ΔT's for the film and coolant in the hottest channel. Thus, $(P/V)_{m'}$ obtained in the above manner, is the value that should be used in establishing the burnout margin.

The results of the heat transfer study indicate that for a coolant velocity of 45 ft/sec, fuel plate and coolant channel thicknesses of 0.040 in. each, active core length 12 in., inlet temperature 120°F, and maximum surface temperature 450°F, it is possible to achieve a maximum power density of 7.2 Mw/liter. The equivalent heat flux is 2.3×10^6 Btu·hr^{-1}·ft^{-2}, and the corresponding burnout heat flux is estimated to be about 5.3×10^6 Btu·hr^{-1}·ft^{-2}.

The McGill-Sibbitt,[7] Buchberg,[8] and Jens and Lottes[9] correlations were used to predict burnout heat flux at reactor mid-plane and exit for both 67- and 100-Mw operation. Extensions of burnout heat flux to the present length-to-equivalent-diameter ratios of 75 and 150 were made, where necessary, by the approximate rule[10] that doubling L/D reduces $(q/A)_b$, the burnout heat flux, by 15%. Results for both burnout heat flux and burnout power density are tabulated below.

	67 Mw	100 Mw
$(q/A)_b$ at outlet end, Btu·hr^{-1}·ft^{-2}	4.62×10^6	4.37×10^6
$(P/V)_b$ at outlet end, Mw/liter	14.4	13.6
$(q/A)_b$ at mid-plane, Btu·hr^{-1}·ft^{-2}	5.45×10^6	5.29×10^6
$(P/V)_b$ at mid-plane, Mw/liter	16.9	16.4

The values given represent the arithmetic average of the three predictions for each case. The maximum ratio of maximum predicted burnout heat flux to minimum predicted burnout flux for any case listed was 1.26. In all calculations, inlet bulk temperature and pressure (above the top of the core fuel region) were taken as 120°F and 665 psia, respectively. Since burnout heat flux data usually vary by about ±35% from the best mean correlation, the maximum design heat flux should be no greater than two-thirds of the predicted burnout value.

Since the maximum expected heat fluxes during 67- and 100-Mw operation are 1.55×10^6 and 2.32×10^6 Btu·hr^{-1}·ft^{-2}, respectively, the ratios of burnout heat flux (two-thirds of the minimum values from the table) to maximum local operating heat flux are as follows:

Power (Mw)	$(q/A)_b/(q/A)_{\text{max local}}$	
	At L	At $L/2$
67	3.2	2.13
100	2.0	1.38

Since the burnout values used are minima above which all data should fall, and since the maximum operating value includes all nuclear and engineering hot channel and hot spot factors, the ratios above represent additional safety margin beyond any foreseen steady-state contingency. However, since there is essentially no operating experience for such high fluxes it is possible that the above values of heat flux are beyond practical limits for subcooled systems. For this reason cooling systems employing other types of fuel elements are being considered for achieving the necessary high power densities.

2.3. Reactor Core

General Description. – The reactor core and pressure vessel are shown in Figs. 13 and 14. The core consists of a central 14-cm-dia light water island, an 11-cm-thick fuel annulus, and a 30-cm-thick beryllium reflector.

As is shown in Fig. 14, cooling water enters the lower section of the reactor pressure vessel at a point just above the lower support plate. A baffle formed by the lower support plate and the outer shim guide cylinder directs the flow upward through the reflector and thermal shield assemblies. The flow continues downward through the

[7] H. L. McGill and W. L. Sibbitt, ANL-4603 (1951) and ANL-4915 (1952).

[8] H. Buchberg *et al.*, Heat Transfer and Fluid Mechanics Institute Reprints, p 177–91, 1951.

[9] W. H. Jens and P. A. Lottes, ANL-4627 (1951).

[10] P. Griffith, MIT, Cambridge, Mass., private communication, Sept. 1957.

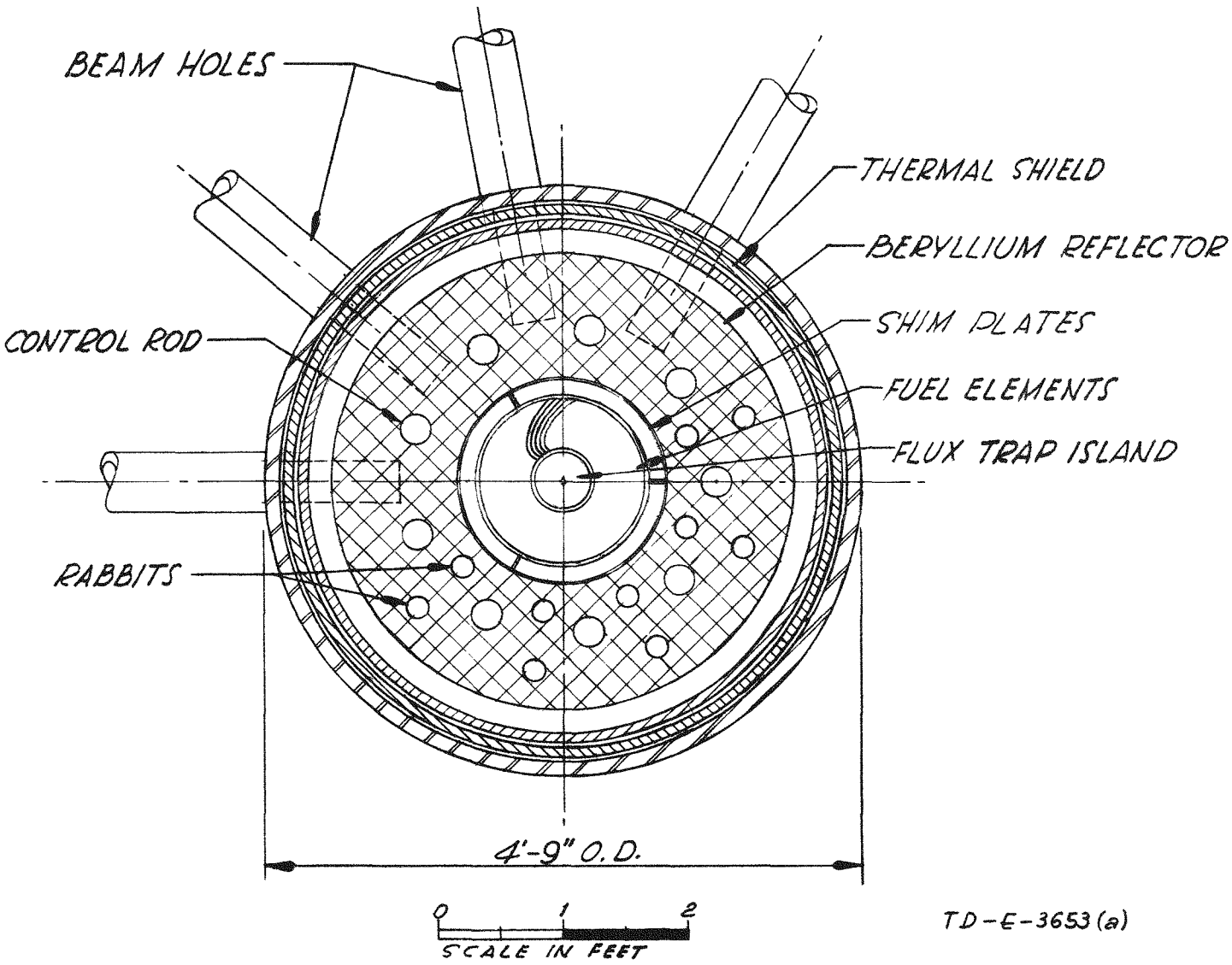

Fig. 13. Reactor Core – Horizontal Section.

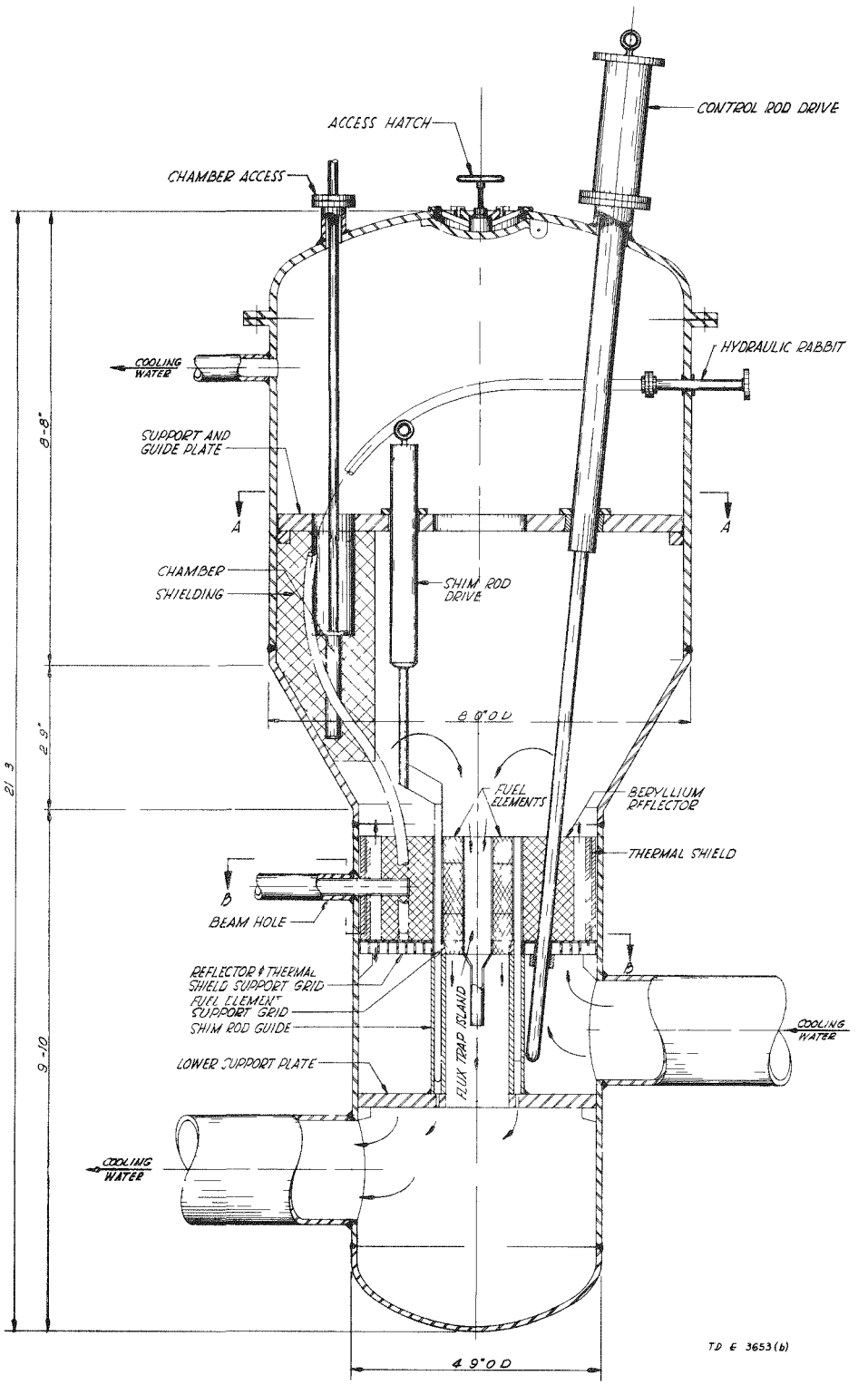

Fig. 14. Reactor Vessel – Vertical Section.

fuel annulus, shim plate region, and flux trap island to the discharge at the bottom of the pressure vessel.

Fuel-Reflector Assembly. – The active lattice as presently conceived consists of curved plate-type fuel elements arranged in an annular ring about the flux trap. The total length of each fuel assembly is 2 ft plus lower end boxes which serve to locate and hold the individual fuel elements in the fuel element support grid. The fuel element support grid, held in place by the lower support plate, serves as a locating device and support for both the fuel elements and the irradiation specimens. These will be affixed at their lower end to an orifice plate. This orifice plate will fit into the central conical section of the fuel element support plate and will control the flow of cooling water both through the irradiation sample and through the remainder of the flux trap.

Immediately adjacent to the outside of the fuel annulus is a 1-in.-thick annulus containing the shim plates. The inner shim plate guide is formed by the fuel array and the cylinder connecting the fuel element support grid and the lower support plate. The outer shim plate guide consists of a cylinder, permanently affixed to the lower support plate, and extending up to the top of the reflector assembly.

The reflector support grid serves to locate the individual pieces of beryllium comprising the reflector assembly. Included in the reflector are nine 3-in.-dia control rod holes, ten 2-in.-dia vertical irradiation holes, four 4-in.-dia horizontal beam holes spaced on 40° intervals, and sufficient coolant channels to ensure adequate cooling of the reflector. Provision will be made for filling any unused experimental holes with beryllium, either by inserting special plugs or by replacing individual reflector units.

Water flow passages and iron thermal shielding are provided at the periphery of the beryllium reflector. The thermal shield will consist of two or three steel cylinders, 2 to 4 in. in total thickness. These will be located and supported by the reflector support grid. The water annuli will provide cooling for the thermal shielding and the pressure vessel wall and will serve as the flow path for most of the cooling water. These annuli will be orificed to ensure adequate coolant flow through the reflector assembly while maintaining as low a pressure drop as possible across it. Calculations indicate that a pressure drop of less than 10 psi across the reflector will provide adequate cooling of the beryllium. Adequate hold-down devices will be provided for the beryllium reflector pieces as required.

Pressure Vessel. – The HFIR pressure vessel, shown in Fig. 14, will be fabricated of stainless steel or stainless-clad pressure vessel steel and designed for a pressure of 700 psi. As shown in the figure, the flanged elliptical head is penetrated by the nine control rod assemblies, which are individually flanged to the top head, and is provided with a 21-in. quick-opening hatch to allow convenient access to the fuel elements and central irradiation facility during shutdown.

Control Mechanisms. – This reactor has been provided with two types of controls: (1) nine rods located in the beryllium reflector for fine control and safety purposes and (2) three shim plates located immediately outboard of the fuel annulus for control of the large excess δk required in the clean condition to obtain reasonably long fuel cycles. The control rods are packaged units, each one being individually flanged to, and removable through, the top head of the reactor pressure vessel. The shim plates, consisting of annular segments, are actuated by drive mechanisms located within the top section of the reactor pressure vessel. The units, including the shim plates, are removable through the hatch in the top head of the reactor tank. The top portion of the shim plates will contain boron or cadmium, and the lower section will be of beryllium. Preliminary investigations show that it may be possible to use boron in the upper section with the concentration adjusted so that the boron will be burned out during operation, and to some extent act as a burnable poison. This idea will be investigated further during detailed design.

2.4. Reactor Structure and Shielding

The reactor unit is located in the center of a hexagonal pool of demineralized water approximately 20 ft across flats and 35 ft deep, as shown in Figs. 15 and 16. A 10-ft-square service pool of the same depth, adjacent to the reactor pool, provides for the storage of fuel elements, tools, reactor components, etc. An 8-ft-wide canal 15 ft deep provides additional storage space for reactor operations and transfer access to the hot cell area in the adjacent building. The service pool and

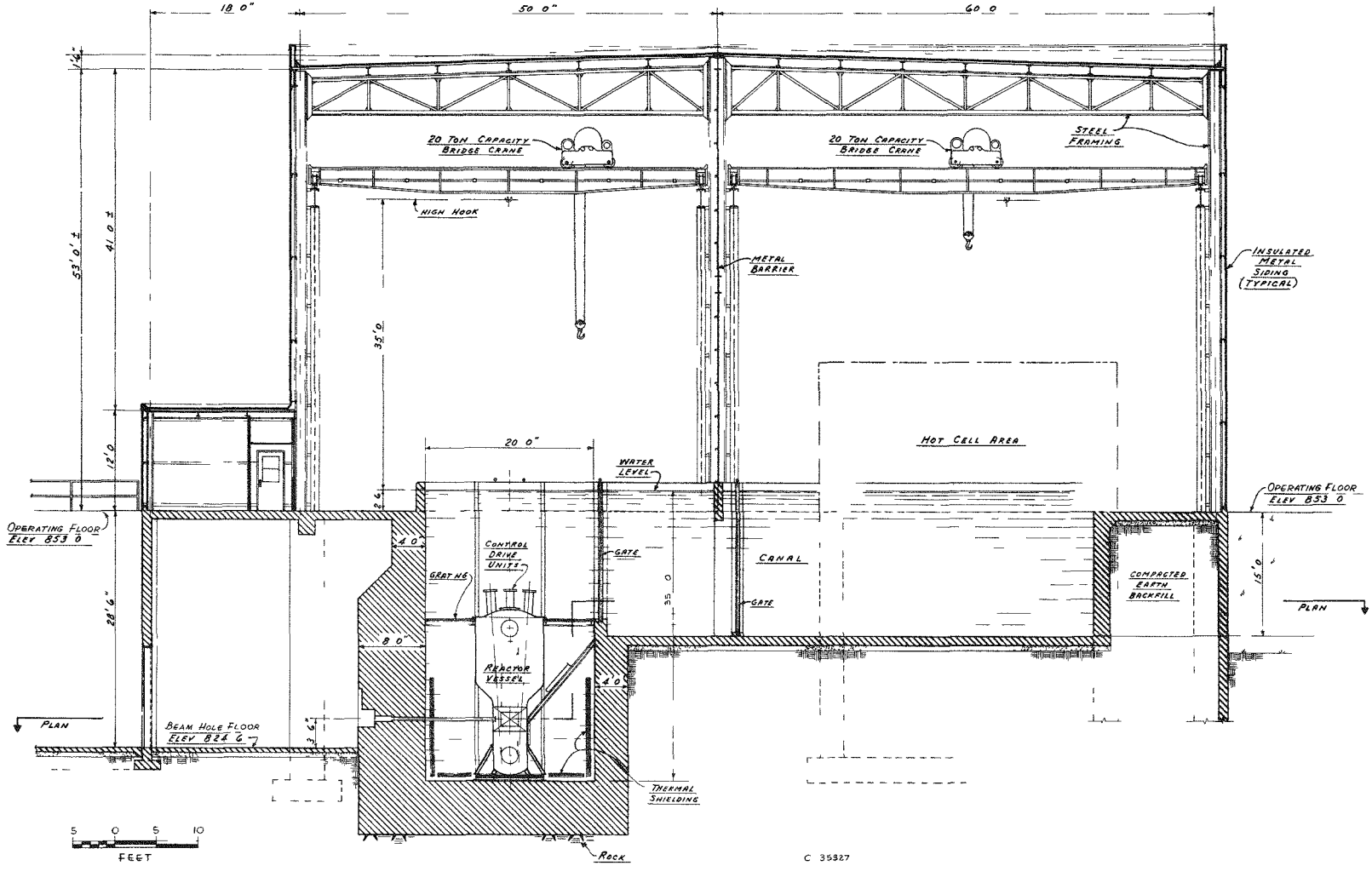

Fig. 15. Reactor and Hot Cell Building – Vertical Section.

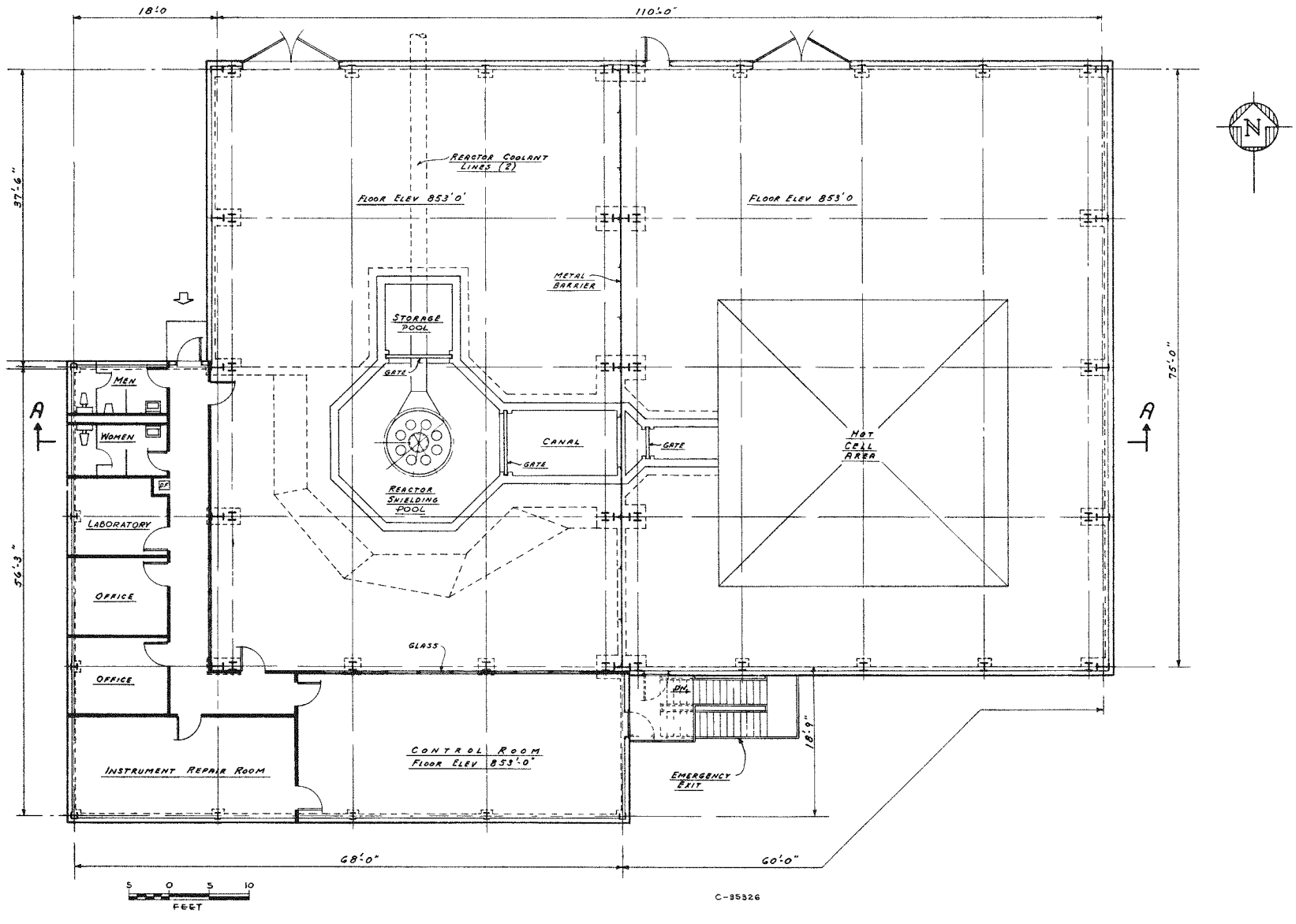

Fig. 16. Reactor and Hot Cell Building – Operating Floor Plan.

canal are separated from the main reactor pool by gate sections which provide for better control of water purity and contamination and which enable the pools to be independently drained. A metallic liner will probably be used to prevent leakage through the concrete pool walls and to assist in the maintenance of high-purity water. Biological shielding above the core is provided by the depth of pool water. Shielding at the beam hole floor level is provided by the water in the pool and the concrete structure. The length of the beam holes from the core to the face of the shield is not considered to be of prime importance in this facility, since the beams must be highly collimated; therefore no effort has been made to minimize the distance between shield face and reactor core. More detailed discussions with experimenters may indicate an advantage accruing from shorter beam tubes, and this will be more carefully considered later. Thermal shielding will be used between the reactor and the inside surfaces of the pool as necessary to prevent excessive temperature gradients in the concrete shield.

The water shielding arrangement allows for flexibility in the installation, operation, and servicing of the reactor unit. Necessary shielding for transfer of fuel elements, reactor components, etc., from the pressure vessel to the storage pools is provided by the depth of water above the top of the pressure vessel. Normal servicing of the reactor, such as the replacement of control rod drive units or hydraulic rabbit tubes, would be accomplished by lowering the water level to the grating at the top of the pressure vessel.

The main coolant line connections to the reactor vessel pass through the solid wall portions of the service pool, continue through the service pool, and then extend underground in a straight line to the pipe trench area of the process water building. Permanent access in the form of a shielded pipe tunnel would be maintained for repair or replacement of these and other pipe lines.

2.5. Experimental Facilities

In view of the fact that this reactor is primarily a facility for heavy element production, the central flux-trap region is considered to be the major experimental facility. In addition to the central facility, however, space in the reflector will be useful for the irradiation of small capsules and samples at relatively high thermal neutron fluxes. The four small-diameter beam tubes terminating in the outer reflector region also provide relatively high beam intensities for basic research investigations requiring collimated beams. It is believed that these secondary facilities will increase the over-all utility of the reactor without seriously compromising the primary objective and without unduly increasing its cost.

In the present concept, the sample configuration for the central facility is that of a cylinder with proper coolant channels and metal-to-water ratios to achieve the maximum flux averaged over its volume. Since the sample configuration to accomplish this will vary with the particular type of sample, its size, and the absorption and fission cross sections, more detailed studies will be carried out to determine the exact arrangement of the materials in the island to maximize the irradiation level and the production rate of heavy elements. Insertion and removal of the sample will be accomplished during shutdown by utilizing the shielding provided by the water in the pool. Present indications are that the samples will generally be in the reactor for long-term irradiation, that is, a year or more. It will be possible, however, to remove the sample easily and transfer it to the hot cell area for inspection for possible corrosion, erosion, or other damage at much shorter intervals.

Ten irradiation facilities are presently proposed in the outer reflector region. These facilities are vertical cylindrical holes penetrating the outer beryllium reflector, each having a nominal diameter of $1\frac{1}{2}$ in. The present concept is to equip each of the holes with a re-entrant-tube hydraulic rabbit installation which will allow for the insertion and removal of samples during operation. The hydraulic rabbit tubes pass through the cover plate or side walls of the reactor vessel near the top and extend along the walls of the canal sufficiently below water level to provide the necessary shielding. Terminal stations are located in the two isotope handling cells, where loading and unloading operations can be done remotely. As the detailed design of the facility proceeds, it is anticipated that additional capsule and sample irradiation facilities will be located in regions farther removed from the core. Provision will be made for inserting and removing holders in these locations with special tools in a manner similar

to that employed for handling fuel elements and the central irradiation samples.

The four beam holes are arranged as shown in Fig. 17. The present concept is to have aluminum beam tube liners which extend from flanged faces at the inside surface of the cubicles to a region separated from the fuel by about 6 in. of beryllium reflector. Outer sleeves of stainless steel which extend from nozzles on the pressure vessel to flanges in the cubicles allow for replacement of the aluminum beam tube liners. The beam tubes are to be located on the horizontal center-line plane of the reactor core and will be 42 in. above floor level. The reactor shield will be arranged so that each beam hole emerges perpendicular to a shield face about 13 ft wide, thus providing adequate space for experimental equipment and shielding. A minimum of 25 ft will be provided between the face of the biological shield and the building wall. The beam hole shown to be pointed west may be extended beyond the building wall for several hundred feet without seriously affecting existing Laboratory installations.

The floor area will be designed for exceptionally heavy floor loadings, as found necessary in previous beam hole experimental equipment design. Since the facility is located on a hillside, the beam hole floor level is also at grade level, although it is 28 ft below the operating floor level.

2.6. Primary Cooling System

The HFIR has a primary and a secondary cooling water system. Heat in the primary system is transferred to the secondary cooling water in a bank of intermediate heat exchangers. This heat is removed from the secondary system in cooling towers. The two systems are shown in the process cooling flow diagram, Fig. 18. The pertinent design data are given in Table 4.

General Description. – In the primary cooling system, approximately 10,000 gpm of H_2O are circulated at a system pressure of 650 psig to permit operation at the design power of 100 Mw. As shown in Fig. 18, the major components are the circulating pumps and intermediate heat exchangers. A decay vessel is located between the reactor and the heat exchangers. Pressurization of the system is obtained by one of two high-pressure feed pumps, the other being an auxiliary. This provides makeup for leakage, seal purging, and the continuous letdown for water treatment. The makeup enters the primary loop at the circulating pump suction, where the loop pressure is about 520 psig during operation. A flywheel on both feed pumps serves to even out pressure and flow variations due to power fluctuation.

A tank is provided for storage of treated water and demineralized makeup. From this tank, water is pumped into the loop by the high-pressure feed pump. A recycle line and pump from the makeup tank to the inlet to the water treatment section provide a means for independent water treatment during reactor shutdown. All components in contact with the primary water are fabricated from stainless steel.

Fuel Region Cooling. – The 650-psig inlet pressure given in Table 4 is based on the use of an additional safety factor of 30°F added on to the maximum fuel element surface temperature to prevent boiling. This maximum surface temperature, 450°F, includes all engineering and nuclear hot spot factors. A heat transfer correlation of the Sieder-Tate type which has been modified by General Electric on the basis of data for plate geometry was used for these calculations. More details of this correlation and the method of calculating the core heat transfer have been given in Sec 2.2.

For pressure drop calculations, it was assumed that the fuel plates are extended vertically upward 4 in. beyond the beginning of the fuel-bearing portion. The extension will provide boundary layer development and stabilization. The parallel flat-plate friction-factor correlation of Rothfus[11] was used in evaluating frictional pressure drop, and a 60-μin. plate surface roughness was assumed. Including end losses of 1.5 velocity heads (maximum) and the effect of heat transfer on viscosity variation, the over-all ΔP is 83.5 psi for the following case:

Radius of flux trap, cm	7
Thickness of fuel region, cm	11
Metal-to-water ratio	1
Velocity, fps	45
Inlet water temperature, °F	120

[11] R. R. Rothfus *et al.*, *A.I.Ch.E. Journal*, p 208–12, June 1957.

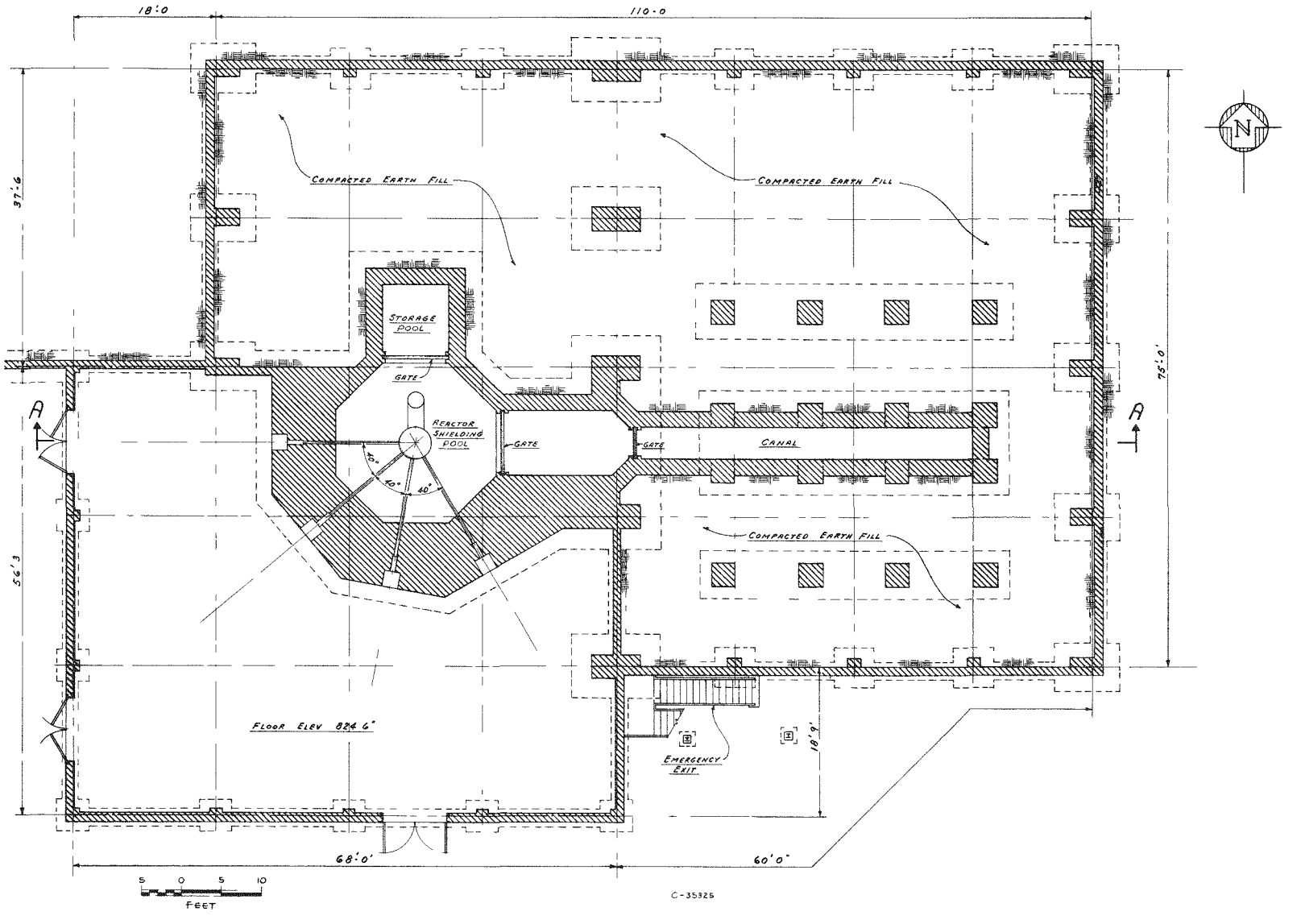

Fig. 17. Reactor and Hot Cell Building – Beam Hole Floor Plan.

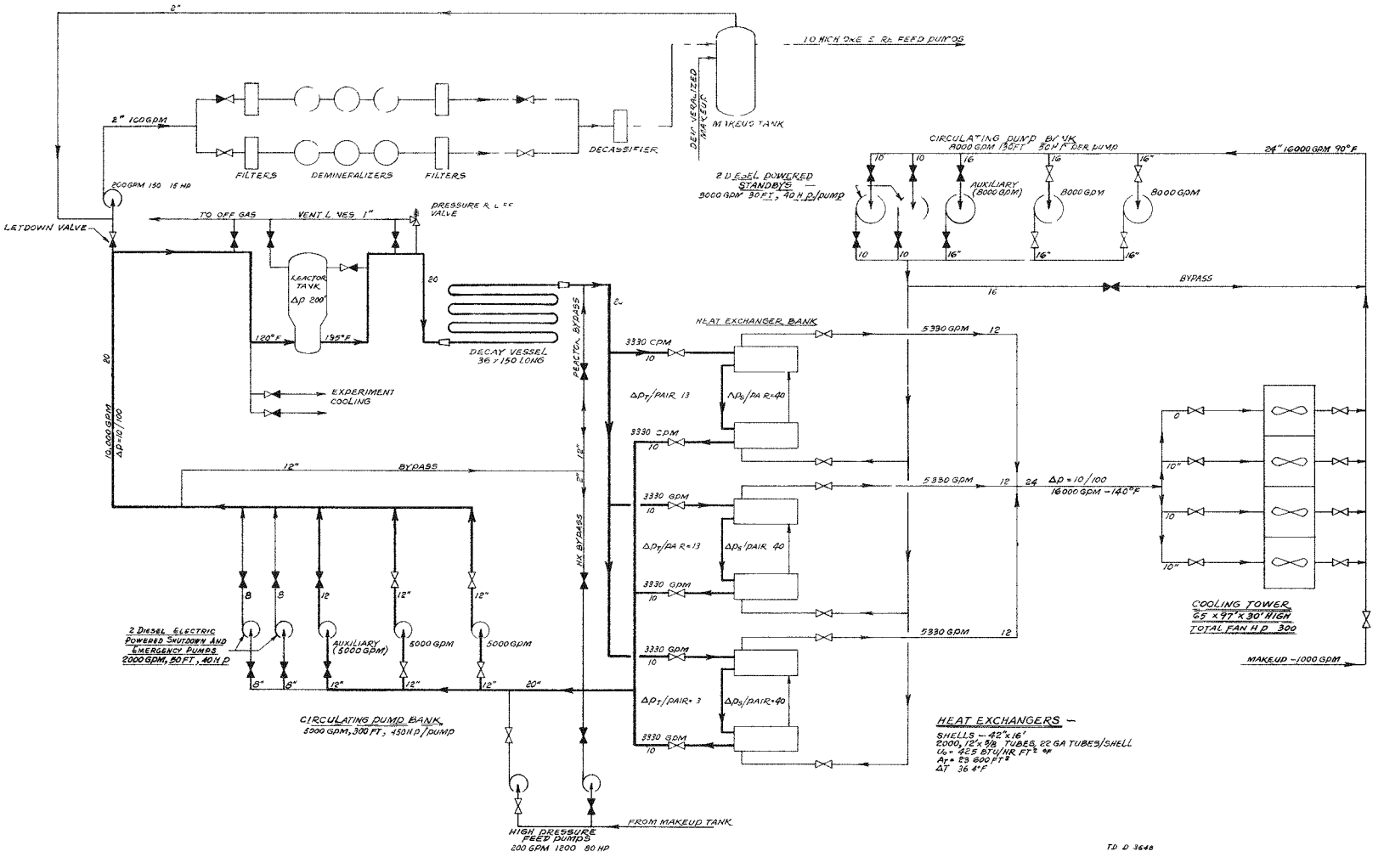

Fig. 18. Process Water System Flow Diagram.

Table 4. HFIR Cooling System Design Data

Parameter	Primary System	Secondary System
Reactor power, Mw	100	
Flow rate (total), gpm	10,000	16,000
Design pressure, psig	700	100
Operating pressure, psig	650	60
Pumping power, hp	900	700
Reactor		
Inlet temperature, °F	120	
Exit temperature, °F	195	
Pressure drop, psi	84	
Flow rate (fuel region), gpm	9400	
Velocity (fuel region), fps	45	
Decay vessel		
Type	Unbaffled pipe	
Holdup time, sec	48	
Dimensions	36 in. ID by 150 ft long	
Heat exchangers		
Type	Shell and tube	
Number	6	
Coolant flow	$\frac{1}{3}$ in series through two units	
Coolant location	Tube side	Shell side
Pressure drop, ft of water	13	40
Inlet temperature, °F	195	90
Exit temperature, °F	120	140
Area, ft^2	23,600	
Over-all heat transfer coefficient, $Btu \cdot hr^{-1} \cdot ft^{-2} \cdot (°F)^{-1}$	425	
Shell diameter, in.	42	
Over-all length, ft	16	
Tube size	$\frac{5}{8}$ in. OD × 0.028 in. wall (22 BWG), 12 ft long	
Number of tubes per shell	2000	
Circulating pumps		
Type	Centrifugal	Centrifugal
Number (including 1 auxiliary)	3	3
Capacity, gpm	5000	8000
Head, ft of water	300	130
Power rating, hp	450	350
Emergency and shutdown pumps		
Type	Centrifugal	Centrifugal
Number (including 1 auxiliary)	2	2
Capacity, gpm	2000	3000
Head, ft of water	50	30
Power rating, hp	40	40

Table 4 (continued)

Parameter	Primary System	Secondary System
Pressurizing and feed pumps		
Type	Centrifugal	
Number (including 1 auxiliary)	2	
Capacity, gpm	200	
Head, ft of water	1200	
Power rating, hp	80	
Cooling tower		
Type		Forced draft
Number		1 (4 cells)
Inlet temperature, °F		140
Exit temperature, °F		90
Fan power (total), hp		300
Face area, ft^2		6300
Dimensions (over-all)		65 ft × 97 ft × 30 ft high
Per cent year-round operation		100
Primary piping		
Size	20 in., sched 40	24 in., sched 10
Pressure drop, ft per 100 ft	10	10
Material of construction	Stainless steel	Carbon steel

For the same flux trap radius but with a 12-cm fuel annulus, the over-all ΔP is 84 psi.

Flux-Trap Region Cooling. – The cylindrical sample region, 4 cm in diameter by 30 cm long, was assumed to have a metal-to-water ratio of 1.0 and a heat dissipation of 50 kw. Calculations for the case where water flows downward under the influence of fuel region ΔP (84 psi) through a single concentric hole of 1.12-in. diameter indicate a velocity of 89 fps, corresponding to a flow rate of 273 gpm, a heat transfer coefficient of ~14,000, a $(\Delta t)_{film}$ of 44°F, and an inner surface temperature of 169°F. For uniform volume heat generation in the annular sample volume and a thermal conductivity of 100 $Btu \cdot hr^{-1} \cdot ft^{-1} \cdot (°F)^{-1}$, the temperature drop across the cylinder wall would be only 52°F with no external cooling. The maximum cylinder temperature would, therefore, be 221°F.

The sample cylinder is obviously overcooled for this case of uncontrolled downward flow. In practice, a pipe attached to the base of the sample-region hole could be sized so as to restrict the flow to any value desired for a particular sample.

Reflector Cooling. – The reactor inlet water flows up through and around the outside of the beryllium reflector, with the bulk of the flow in the outside annulus, resulting in a pressure drop through the beryllium less than 10 psi. No difficulty is expected in cooling the beryllium with the specified pressure drop and coolant volume. Preliminary calculations show that for a power density of 50 w/cc, a coolant channel diameter of $\frac{1}{4}$ in., and an annular geometry, the maximum beryllium temperature will be less than 200°F.

Decay Tank. – A decay vessel is located after the reactor. The 36-in.-ID × 150-ft unbaffled unit has a capacity of 8000 gal. This provides a holdup time of 48 sec, for the decay of the N^{16}.

Intermediate Heat Exchangers. – Three sets of heat exchangers are connected in parallel. Each set consists of two exchangers in series flow. The primary coolant flows through the tubes. Secondary water enters the shell side of the exchangers at 90°F and leaves at 140°F. The mean temperature difference is 36.4°F, the over-all coefficient is 425 $Btu \cdot hr^{-1} \cdot ft^{-2} \cdot (°F)^{-1}$, and the total heat transfer area is 23,600 ft^2. The design of the heat exchangers has been based

on commercially available sizes. With a 42-in. shell, over-all lengths are 16 ft. Tube sizes are $\frac{5}{8}$ in. OD by 0.028 in. wall (22 BWG), 12 ft long.

Circulating Pumps. – Two 5000-gpm, 450-hp circulating pumps provide the coolant flow at design power with an available pressure drop of 300 ft of water. An auxiliary 5000-gpm, 300-ft, 450-hp pump is connected in parallel with the first two. This allows the reactor to operate at design conditions when one pump is down for maintenance. Two 2000-gpm, 50-ft, 40-hp auxiliary standby pumps are provided for emergency and shutdown cooling.

2.7. Secondary Cooling Systems

Water at essentially atomspheric pressure is used as the coolant in the secondary system. Total required flow at reactor design power is 16,000 gpm. The basic components of the system consist of the intermediate heat exchangers, a forced-draft cooling tower, and the circulating pumps, with a bypass on the pumps. Makeup to the system is put into the basin of the cooling tower. Chemical water treatment is done by the addition of the chemicals at the cooling tower. The basic material of construction is carbon steel.

Two 8000-gpm, 130-ft, 350-hp pumps provide the required coolant flow rate of 16,000 gpm. An additional pump is installed as an auxiliary. Shutdown and emergency cooling is provided by two (one standby) 3000-gpm, 30-ft, 40-hp pumps which are powered by both auxiliary (diesel) and electrical power.

Flow is then through the shell side of the intermediate heat exchangers, with parallel flow through three sets of two connected in series. Each heat exchanger pair acts effectively as a four-tube-pass, two-shell-pass unit. No extra heat exchanger capacity for auxiliary purposes has been provided, as relatively maintenance-free operation is expected. The temperature rise through the units is 50°F, that is, from 90 to 140°F, with a 40-ft pressure drop.

The coolant approaches the forced-draft cooling tower at 140°F and discharges at ~90°F. The installed capacity of the cooling towers is such that year-round operation will be possible. No extra capacity has been provided for operation at greater design power or for maintenance auxiliary. The cooling tower is 65 ft × 97 ft × 30 ft high with 6300 ft^2 of face area. Makeup requirements are 1000 gpm, and the total fan horsepower is 300.

Emergency Cooling. – Auxiliary pumps have been provided for emergency reactor cooling in both the primary and secondary systems in the event of electrical power loss. These will be powered by both auxiliary power (diesel) and electrical power, the electrical power being used for normal shutdown cooling. It is expected that with flywheels attached to the circulating pumps, sufficient flow will be maintained, in the event of a power loss, while the auxiliary pumps are brought on line.

No provision for auxiliary power of the pressurizing pumps has been made, though with flywheels attached to the pumps it is expected that the required pressurization will be maintained until the reactor power has been reduced to a level at which the danger of boiling in the fuel region is minimized.

Possible means of emergency cooling in the event of a rupture in the primary system are:

1. a spray system installed in the reactor tank,
2. loops in the reactor coolant inlet and exit lines which maintain the reactor flooded with water, and which require vents in both lines to break any siphon effect, and
3. a drain line and reactor tank valve which make it possible to drain the pool water through the reactor fuel region.

2.8. Buildings

Reactor Building. – The reactor building consists of the reactor, storage and transfer pools, and the volume enclosed by the structure above the 50 × 75 ft reactor operating floor; the height is determined by the minimum 35-ft crane hook clearance necessary to allow for ease in handling materials located on or near the bottom of the pools. The degree of containment necessary to assure against possible accidents has not been evaluated at this time and cannot be until a detailed investigation is made. However, the proposed arrangement, based on ORR-type containment, can be easily modified to provide complete containment at a minimum cost. No direct access is provided from the reactor room to the adjacent control room, office wing, beam hole experimental areas, or the adjoining hot cell and isotope handling building. Truck access

is provided from a roadway area to the north. A water barrier is used in the canal entrance to the hot cell building to prevent air circulation and provide some degree of isolation; this degree of isolation can easily be changed as more detailed criteria are established. Floor loading design will be based on necessary requirements for handling and storage of shielded carriers and other operations equipment.

A minimum of floor space for the operating staff and control room is located at the same elevation as the main reactor floor level and directly over the beam hole experimental areas. Access to the offices and control room is available through the corridor without entry to the reactor building. A common emergency exit is provided for the control room and the rear of the hot cell building.

Process Water Building. – Figure 19 is a horizontal section through the shielded cell area of the process water building, showing an arrangement of the major pieces of equipment for the reactor and pool cooling and demineralizing systems. The floors of the cells are at grade level, with access being provided by the removal of shielded block walls, offset personnel entrances, or roof slabs, depending upon service and inspection requirements. A 10-ft-wide shielded pipe gallery common to all cells at this elevation provides for interconnections, valving, and instrumentation. An underground tunnel, possibly with permanent access, connects this pipe gallery with the reactor building.

The floor above the process water equipment cells is used for the electrical distribution center, pump starters, air conditioning equipment, secondary cooling system chemical treatment equipment, etc. The control center for the process water system, providing for manual operation of valves and equipment which are infrequently used, is in this area. It is planned that those operations which are vital and necessary in routine operation of the system will be controlled from a small graphic panel in the reactor control room in order to more efficiently integrate the over-all operation of the facility.

The building structure above this floor is of inexpensive construction, providing only weather protection. Provision will be made for crane service in those areas where cell roof slab or heavy equipment handling is necessary.

Hot Cell Building. – The hot cell building, although sharing a common wall with the reactor building for economy in construction, is considered a separate and distinct isolation area. Its 60×75 ft floor area is regarded as the minimum required for the installation of two special purpose isotope handling cells and one general purpose cell. These cells will be designed primarily to ease the problems of loading and unloading radioactive samples. The hydraulic rabbit tubes will terminate in the two isotope handling cells, thereby making it relatively easy to load samples into transfer casks to be taken to other facilities for processing. It is planned to incorporate a decontamination and cell servicing area within shielding in order to minimize the spread of any radioactive contamination that might result from sample failures. Details of cell arrangement cannot be presented without additional study, although it is generally agreed that existing laboratory designs modified to incorporate pool transfer features are adequate.

The building construction will be simpler in design than that of the reactor building; it is probable, however, that some form of activity confinement features will be incorporated.

Truck and personnel access will be provided at grade level, as in the reactor building. An overhead crane will be provided for handling the hot cell shielding and for transfer casks.

2.9. Facility Location and Arrangement

The proposed location for this reactor facility is shown in Fig. 20, which is a plant layout drawing of the Oak Ridge National Laboratory. The indicated site and the area to the west of it have been reserved as a reactor area in the plant planning program for several years. There are several other possible locations for the reactor, and these will be carefully evaluated before a final decision is made; the proposed site, however, appears to be the best choice at present.

The Laboratory center is shifting to the east as far as general office and laboratory space are concerned, and the 4500 area, as indicated on this plan, is the administrative, office, and laboratory area. Contracts have been let for approximately $10 million to provide additional office and laboratory space in the 4500 area. The site selection, therefore, is consistent with the over-all plan to separate operations involving the handling of large

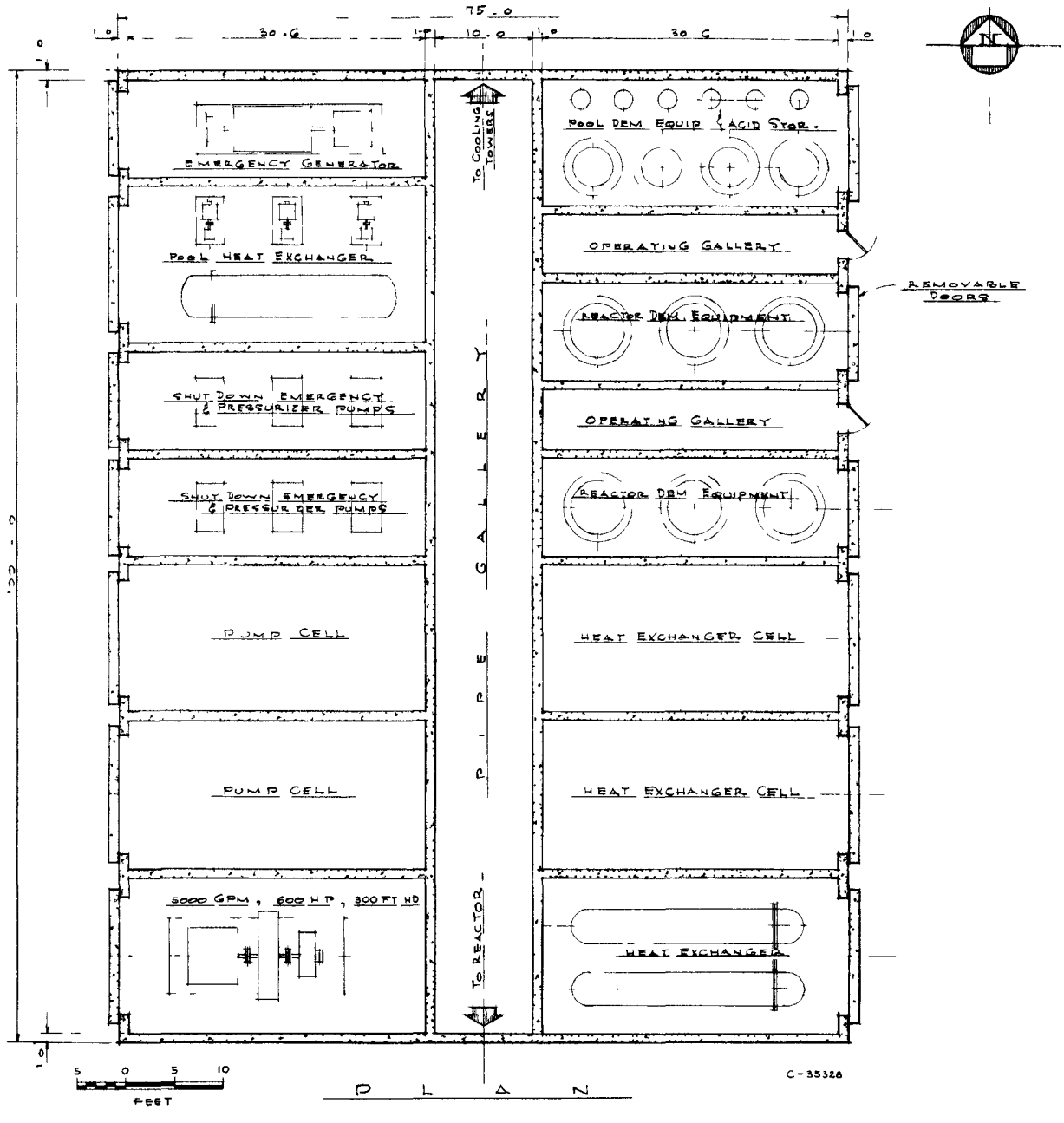

Fig. 19. Process Water Building Layout.

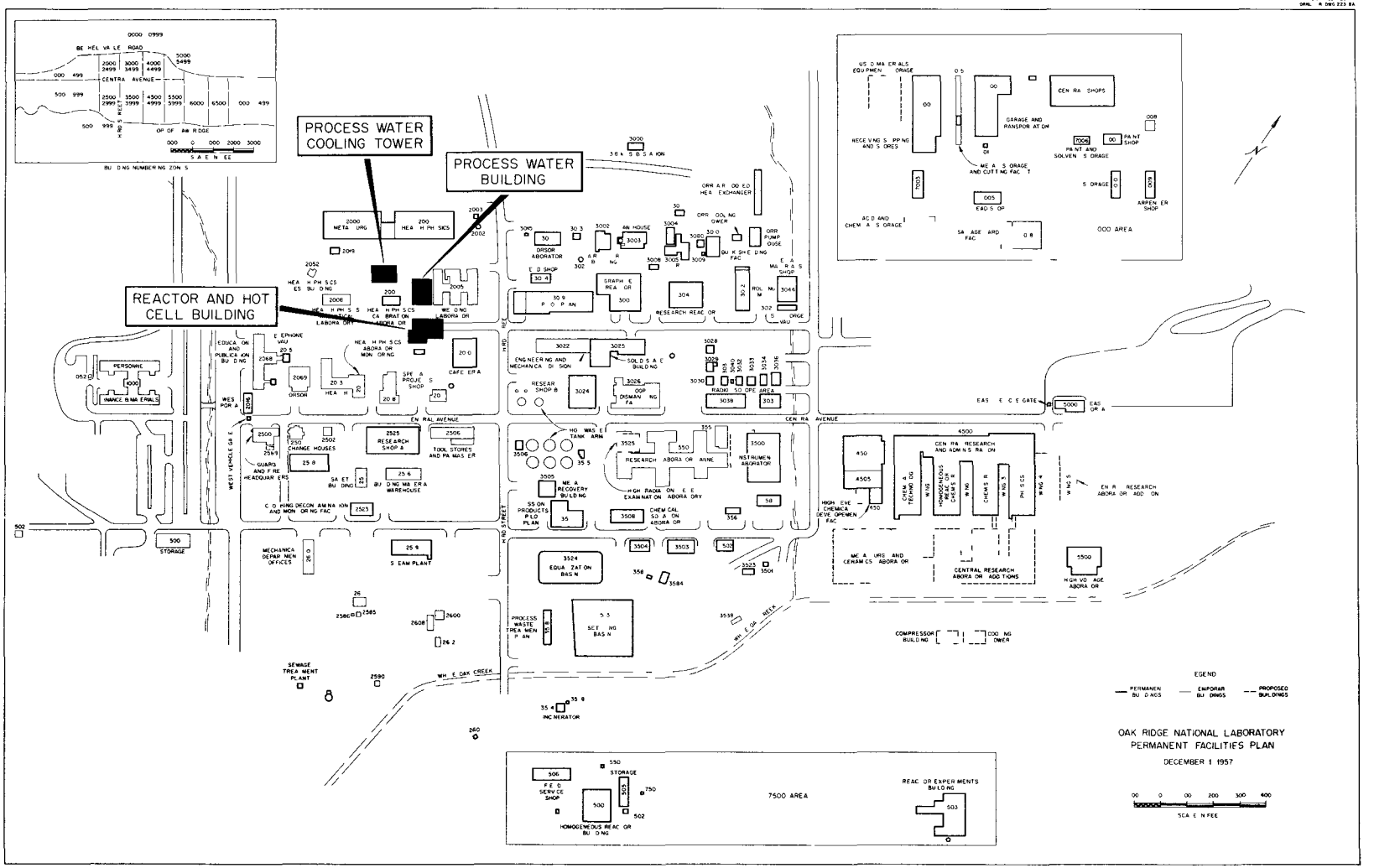

Fig. 20. Laboratory Site Plan.

quantities of radioactive materials from the normal office and laboratory functions.

In this proposed location the land slopes down from Hilltop Circle toward Central Avenue, and therefore the location is advantageous for a building to which grade access is desirable from several levels. In addition, the area selected is conveniently located with respect to services such as waste disposal, power, and water. The short distance (approximately 150 yards) from other reactor installations will allow the Operations Division to utilize their operating personnel and equipment more efficiently, thereby reducing the operating costs to a minimum.

It is planned to convert an existing cafeteria, Building 2010, to provide space for offices and laboratories needed by the Operations Division. Thus a minimum of such space will be needed in the new facility; this is considered highly desirable from the standpoint of control of possible contamination.

In considering the many possibilities for arrangement of the facility, the conclusion has been reached, on the basis of the operating experience of the Reactor Operations Division and the Isotope Division, that contamination can and will occur as a result of handling materials in and around reactors. This has led to the arrangement shown in Fig. 21, in which the reactor building, the beam hole building, the hot cell and isotope handling building, the office and control room space, and the process water building will be separate areas in so far as this is practical. Each of these areas will be a separate enclosure with respect to ventilation, truck access, and personnel access, and each will be designed to provide the degree of containment judged to be adequate for the particular operations that will be carried on in that area. This principle of isolation has been successfully used in the Isotope Division for years and has been proved to be a sound approach.

3. REQUIRED RESEARCH AND DEVELOPMENT

3.1. Critical Experiments

Critical experiments with flux-trap geometries are being planned as part of a program of general research and development for ultra high flux reactors. Arrangements applicable to the design of the HFIR will be investigated in this program along with other systems, providing data necessary for final optimization of the HFIR core. The effect of varying the geometry of the sample exposed in the central irradiation facility on the achievable thermal flux will be of particular interest in these studies. Temperature coefficients of reactivity will also be determined as a basis for specifying control system requirements.

In the experimental program as now planned, highly enriched U^{235} in solution will be contained in an annulus formed by two concentric cylindrical tanks. Water and other materials, such as neutron absorbers or beryllium, will be placed in the inner tank, and the entire assembly surrounded by a good reflector of beryllium, D_2O, or graphite. Each assembly will be made critical by varying the concentration of the U^{235} in the fuel region. Foils will be irradiated in the various regions to determine the neutron flux distribution.

In addition to the critical experiments required to provide data necessary for the conceptual design of the HFIR, a critical assembly simulating or duplicating the final design will probably also be required because of the unique arrangement and performance characteristics of the reactor.

3.2. Fuel Element Development

The development of fuel elements capable of operating at maximum power densities up to 7500 kw/liter and average power densities up to 4000 kw/liter is desirable in order to achieve the maximum thermal neutron flux at minimum total power levels in the HFIR. At this time, one type of fuel element shows promise for achieving such performance. This fuel element utilizes 30- to 50-mil plates spaced 30 to 50 mils apart, suitably curved to permit complete filling of the annular fuel region. Both dispersion and alloy fuels will be considered for the fuel-bearing portion of the plates, with either aluminum or stainless steel cladding. For highest performance, moreover, a method of varying the U^{235} concentration across the width of the plate to flatten the radial power distribution must also be developed.

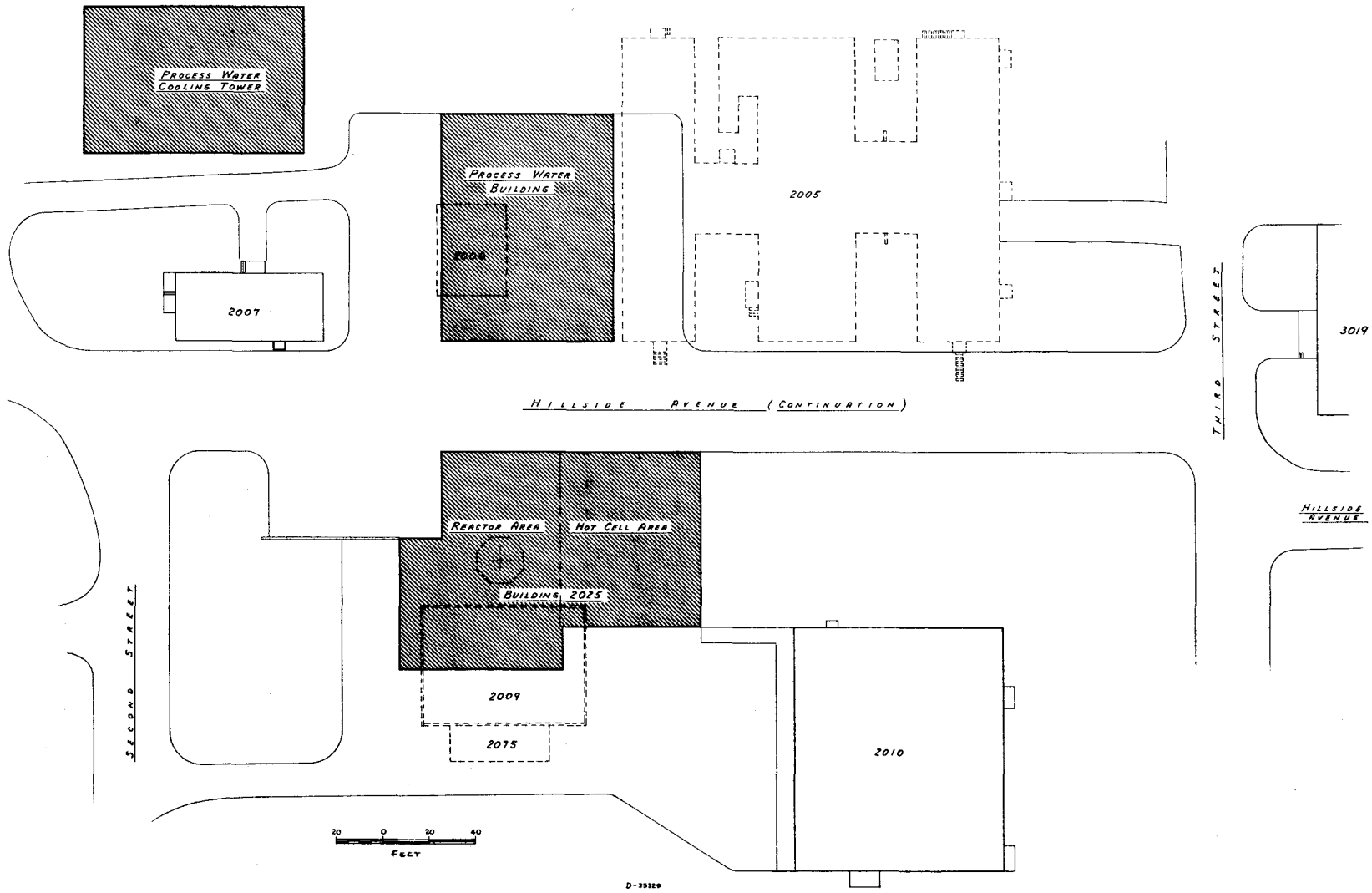

Fig. 21. Building Site Plan.

A research and development program to investigate the general field of high-power-density fuel elements has been proposed. The results of this program will for the most part be specifically applicable to the design of HFIR fuel elements.

3.3. Engineering Experiments

Hydraulic Tests. – The two-pass flow of coolant water presently planned should involve few problems of flow distribution between various regions of the reactor. During the first pass, all the primary water flows vertically upward through core components having relatively small heat generation rates – the thermal shield and beryllium reflector. These regions will be overcooled, and the margin for error in flow distribution will be large. Following coolant reversal at the top of the core, the total flow will pass vertically downward through the fuel annulus, sample cylinder, water island, and shim plates. The planned flow rate is sufficient to ensure a 45-fps velocity in the fuel region and more than adequate cooling for the sample and island (based on 50-kw heat generation in the sample).

Because of the large power density and heat flux necessary in the fuel annulus, it is felt that studies of flow distribution between individual channels and across the fuel annulus radius are necessary. Any observed flow maldistribution would be intimately related to the engineering hot channel factor, taken as 1.7 in the present design. This factor may have to be modified according to the results of the studies of flow gap variation and flow distribution. Since the axial and radial variations of heat generation rate are everywhere the same for the symmetrical fuel annulus (within a tolerance established by variation in fuel loading), and since the pressure drop across the fuel region is relatively large, good flow distribution is expected.

To ensure a stable and hydrodynamically established boundary layer at the tops of the heated portions of the fuel plates, it is desirable to extend the plates (without fuel) approximately 4 in. A simple flow test would indicate the adequacy of such a plate extension.

The only uncertainty with respect to fuel region pumping power which should be investigated is the effect of relative roughness on pressure drop. As was pointed out by Lancet in a recent paper,[12] channels of very small equivalent diameter will act like rough channels unless special care is taken to ensure a smooth surface. Lancet's results show a 132% increase in friction factor above smooth-surface data for a channel for which a 3% increase would be predicted from standard correlations. This very large discrepancy dictates caution in accepting Lancet's data, but a possible problem area is indicated.

Fuel Element Behavior. – The mechanical stability of the fuel plates under the influence of impact head, frictional pressure drop, and possible flow-induced lateral vibration should be determined by experiment.

Heat Transfer Measurements. – To duplicate the large heat fluxes necessary in the fuel region, it would be necessary to conduct tests under high pressure to prevent local boiling. The basis of selection of the equation for heat transfer coefficient has already been discussed; it is felt that this relation is adequate for the present reactor design and that only spot checks on a small and simple model are required. The possible surface roughness effect mentioned above would increase the heat transfer coefficients above those used (but the increase in friction factor would be larger).

Should aluminum be further considered as a cladding material, short-time tests of electrically heated fuel plates operating under design heat flux and coolant velocity would yield valuable data relative to surface corrosion-erosion and possibly needed fuel plate fouling coefficients.

The heat transfer tests should be terminated by burnout studies to indicate the seriousness of such a failure and to establish a more accurately known level of burnout power density.

3.4. Instrumentation and Control System

The main instrumentation problems appear at this time to be those concerned with providing assurance that adequate cooling is present for the reactor core and experimental facilities. This concern is a natural consequence of the fact that

[12] R. T. Lancet, Am. Soc. Mech. Engrs., Paper No. 58-A-122 (1958).

the heat transfer rate has been pushed very high in order to minimize the reactor power level needed to achieve the desired flux. It is not anticipated that a great deal of development work will be required for instrumentation of this type; the project will require, however, a considerable amount of careful engineering of the instrumentation for process water control.

Nuclear instrumentation does not appear to require an effort much greater than that normally expended on a reactor of the MTR-ORR type. It is however, considered highly desirable to investigate the application of modern techniques in electronics, such as solid state devices (transistors), in order to reduce maintenance problems and to give added assurance against unnecessary shutdowns.

An additional complication brought on by the extremely high power densities and the small size of the reactor core is the problem of control rod location. This problem resolves itself into one of obtaining sufficient control of k in the machine and at the same time not unduly perturbing the flux distribution in the fuel region. The approach to this problem is to locate a number of control rods in the primary reflector close enough to the core to exercise sufficient control during normal operation at power and yet far enough removed so that the power distribution in the core is not seriously changed as a function of rod position. In order to obtain a greater control of k to provide for a reasonable safety margin, additional control rods will be located very close to the fuel region, as previously mentioned.

Nuclear calculations for certain core configurations have shown the possibility of a positive temperature coefficient of reactivity associated with the temperature of the water cooling the fuel elements. At the present time there is not a great deal of information available on this matter; however, every effort will be expended to investigate this in greater detail, in the form of both calculations and critical experiments. If the coefficient for rapid increases in temperature is not negative, it may be necessary to take an entirely new approach on the control system, and this would require an extensive effort in terms of research and development.

4. CONSTRUCTION SCHEDULE AND COST ESTIMATE

4.1. Schedule

Present information from the AEC indicates that design and construction funds cannot be made available before July 1, 1960. The schedule given in Table 5 is based on the premise that funds will be made available for conceptual design studies and for research and development work on July 1, 1959. Design criteria, therefore, should be in good order by July 1, 1960, and it should be possible to retain an architect-engineer immediately upon availability of funds for this purpose.

If it is decided that it is necessary to complete the project in a shorter period of time than the schedule indicates, it will be necessary to change the proposed method of handling this project. One method which has been successfully used for handling a project of this type in order to achieve faster completion is to retain a combined architect-engineer and construction contractor on a cost-plus-fixed-fee contract. A contract of the cost-plus-fixed-fee type would probably result in

Table 5. Design and Construction Schedule

Description	By	Start	Completion
Facility design criteria	ORNL	July 1959	July 1960
Reactor component design	ORNL	August 1960	August 1961
Facility design	Architect-engineer	August 1960	March 1961
Construction and installation	Contract	April 1961	October 1963
Initial testing and operation	ORNL	October 1963	May 1964

some increase in cost, which would have to be balanced against the advantages of earlier completion.

4.2. Cost Estimate

The total cost of the HFIR, including the reactor building and supporting facilities, is estimated at this time to be $12 million. The estimates given in Table 6 are based on construction costs at Oak Ridge and are extrapolated from experience in building the 20-Mw Oak Ridge Research Reactor.

Table 6. Cost Estimate

Item	Contract	ORNL	Total
A. Engineering, design, and inspection (12% of construction costs)	$ 745,000	$ 425,000	$ 1,170,000
B. Construction costs			
1. Land and land rights			
2. Improvements to land	100,000	25,000	125,000
3. Building			
a) Structure	900,000		900,000
b) Services	700,000		700,000
4. Other structures			
a) Structure	100,000		100,000
b) Services	80,000		80,000
c) Equipment	1,000,000	500,000	1,500,000
5. Utilities	1,000,000	50,000	1,050,000
6. Equipment and installation	4,275,000	1,000,000	5,275,000
7. Removal costs less salvage			
C. Contingency (10% of A through B)	900,000	200,000	1,100,000
D. Total	$9,800,000	$2,200,000	$12,000,000

APPENDIX

Letter from J. H. Williams to A. M. Weinberg, December 12, 1958, Summarizing Results of High Flux Research Reactor Meeting

I would like to thank you for your participation in the November 24 meeting in Washington on high flux research reactors. Your advice and suggestions will be of great help to us in our high flux research program planning.

I was especially pleased that all of the recommendations and conclusions expressed at the meeting received the unanimous support of the participants.

It is my understanding that agreement was reached on the following points:

1. *Flux regions.* Plans should be made for construction of reactors in the $3–5 \times 10^{15}$ flux region. While for certain uses, fluxes in the 10^{16} range are very desirable, current technology is only adequate for construction of reactors in the $3–5 \times 10^{15}$ flux region. Development of concepts for high fluxes should be continued with support from the Division of Reactor Development.

2. *Types of reactors.* Emphasis should be given to reactors designed to be most suitable for specific research areas rather than to a reactor which would attempt to satisfy all needs. There are needs for: (a) A high flux (flux-trap type, $3–5 \times 10^{15}$ n/cm^2sec) reactor for isotope production, of primary interest to the chemistry program; this reactor can be designed now and is estimated to cost approximately $10 million. (b) A larger reactor providing adequate volume for numerous beam holes for physics experiments; this reactor (flux of the order of $3–5 \times 10^{15}$) is estimated by ANL to cost approximately $30–$35 million, and will require some (year or more) further development.

3. *Plans.* (a) *Isotope producer* – It was unanimously agreed that an isotope producer reactor be designed and constructed at ORNL. This decision on location was based on (1) availability of fuel reprocessing facilities, (2) availability of facilities for processing and distributing the products of the irradiation, (3) the recognition that ORNL is a national center for isotope research and development, and (4) interest in the laboratory in constructing the reactor. This reactor would serve as the first AEC-wide high-flux facility and be operated in conjunction with the national heavy element production program. In anticipation of the inclusion of a construction request for this reactor in the FY 1961 budget, a meeting will be held in two or three months in order to discuss in further detail the design, facilities, and use of the reactor. (b) *Physics reactor* – Argonne will explore with the Division of Reactor Development support for design and development of the multi-purpose reactor (type (b) of paragraph 2). After the development period, ANL may submit a proposal to the Division of Research. It should be noted that the ANL development studies will also be of use in the subsequent development of a 10^{16} flux "barrel of neutrons."

Thank you again for your interest and cooperation. I would be pleased to receive any further comments or recommendations you may care to make.

BIBLIOGRAPHY ON FLUX-TRAP REACTORS

Alichanow, A. I., *et al.*, "A Heavy Water Research Reactor," *Proc. Intern. Conf. Peaceful Uses Atomic Energy, Geneva, 1955*, **2**, 331.

ASTRA, *Advanced Engineering Test Reactor*, 20 E 1.1.

Babcock & Wilcox Company, Lockheed Aircraft Corporation, *Proposal for an Engineering Test Reactor*, June 30, 1955.

Bolger, J. C., S. F. D'Urso, and R. O. Maak, *Feasibility Study of Superflux Reactor*, EPS-X-293 (December 1956).

Carter, W. L. (group leader), *Design Study of an Advanced Test Reactor* (ORSORT study), ORNL CF-57-8-5 (August 1957).

Cheverton, R. D. (group leader), *High Flux Research Reactor* (ORSORT study), ORNL CF-56-8-206 (August 1956).

Cheverton, R. D., *Further Studies of a D_2O Moderated High Flux Research Reactor* (to be published).

Choudhury, J., *Critical Calculations for the Core of a Very High Flux Research Reactor*, Geneva Conference Paper 1503, August 1958.

Ergen, W. K., *Flux Distribution in a Reactor Consisting of a Spherical Shell of Fuel in an Infinite Moderator*, ORNL CF-57-12-100 (December 24, 1957).

Ergen, W. K., *Fluxes Obtainable in a Flux-Trap Reactor*, ORNL CF-58-1-4 (January 15, 1958).

Ergen, W. K., *High Thermal Neutron Flux from Fission. Oversimplified Cases*, ORNL CF-58-2-127 (February 26, 1958).

Ergen, W. K., *Homogeneous High-Flux Reactor*, ORNL CF-58-3-68 (March 31, 1958).

Feinberg, S. M., *et al.*, *Uranium-Water Intermediate Reactor Used for Obtaining High Intensity Neutron Fluxes*, Geneva Conference Paper 2142, 1958.

Fowler, T. B., *Maximum Thermal Flux per Mw in Three-Region Homogeneous Reactors*, ORNL CF-58-3-76 (March 18, 1958).

Francis, T. L., *et al.*, "A Flux-Trap Reactor for Advanced Engineering Tests," *Trans. Am. Nuclear Soc.* 1(1) (June 1958) (abstract).

Kasten, P. R., M. I. Lundin, and C. L. Segaser, *Aqueous Homogeneous Research Reactor*, ORNL-2256 (April 1957).

Kelber, C. N., *The Theoretical Physics of the Argonaut Reactor*, ANL-5710.

Leyse, C. F., *et al.*, *High Flux Reactors for University Research*, Internuc-22 (March 1958).

Leyse, C. F., *et al.*, *An Advanced Engineering Test Reactor*, Internuc-23 (see also AECU-3427 and Addendum for preliminary report).

Leyse, C. F., *et al.*, "A High Flux Pool-Type Research Reactor," *Trans. Am. Nuclear Soc.* 1(1) (June 1958) (abstract).

Link, L. E., *The Mighty Mouse Research Reactor. Preliminary Design Study*, ANL-5688.

Link, L. E., *et al.*, *Design of a High Flux Research Reactor – Mighty Mouse*, Geneva Conference Paper 423, June 1958.

Nestor, C. W., Jr., *Flux Peaking in Homogeneous Reactors*, ORNL CF-57-8-84 (August 1957).

Osredkar, M., and R. Stephenson, *Thermal Flux in the Central Moderator Zone of Thermal and Fast Reactors*, Geneva Conference Paper 2411, August 1958.

Phillips Petroleum Company, *Cobalt-60 Production Reactor*, IDO-16421.

Ribaric, M., *The Design of Spherical Shell Reactors*, Geneva Conference Paper 475, August 1958.

Stewart, H., *et al.*, "Low-Power Thermal Test Reactor for Nuclear Physics Research," *Nucleonics* 11(5), 38.

U.S. Atomic Energy Commission, San Francisco Operations Office, *Design Requirements for the Livermore Pool Test Reactor*, May 1955.

External Transmittal Authorized
ORNL
Central Files Number
59-2-65

DISTRIBUTION

1. D. S. Billington
2. F. T. Binford
3. E. P. Blizard
4. E. G. Bohlmann
5. G. E. Boyd
6. R. B. Briggs
7. A. D. Callihan
8. R. A. Charpie
9. A. Chetham-Strode
10. R. D. Cheverton
11. H. C. Claiborne
12. T. E. Cole
13. J. A. Cox
14. J. H. Crawford
15. W. K. Ergen
16. J. L. Fowler
17. W. R. Gall
18. W. R. Gambill
19. J. P. Gill
20. E. Guth
21. J. A. Harvey
22. N. Hilvety
23. D. K. Holmes
24. W. H. Jordan
25. P. R. Kasten
26–86. J. A. Lane
87. H. A. Levy
88. M. I. Lundin
89. R. N. Lyon
90. R. L. Macklin
91. H. G. MacPherson
92. F. C. Maienschein
93. J. R. McWherter
94. P. M. Reyling
95. M. T. Robinson
96. A. F. Rupp
97. H. C. Schweinler
98. M. J. Skinner
99. A. H. Snell
100. R. W. Stoughton
101. J. A. Swartout
102. E. H. Taylor
103. D. W. Vroom
104. A. M. Weinberg
105. G. C. Williams
106. C. E. Winters
107. E. O. Wollan
108. ORNL – Y-12 Technical Library, Document Reference Section
109. Central Research Library
110–111. REED Library
112–146. Laboratory Records Department
147. Laboratory Records, ORNL R.C.
148–162. Technical Information Service Extension